

Design of Substituted Imidazolidinylpiperidinylbenzoic Acids as Chemokine Receptor 5 Antagonists: Potent Inhibitors of R5 HIV-1 Replication

Renato Skerlj,^{*,†} Gary Bridger,[§] Yuanxi Zhou,[§] Elyse Bourque,[†] Ernest McEachern,[§] Markus Metz,[†] Curtis Harwig,[§] Tong-Shuang Li,[§] Wen Yang,[§] David Bogucki,[§] Yongbao Zhu,[§] Jonathan Langille,[§] Duane Veale,[§] Tuya Ba,[§] Michael Bey,[§] Ian Baird,[§] Alan Kaller,[§] Maria Krumpak,[§] David Leitch,[§] Michael Satori,[§] Krystyna Vocadlo,[§] Danielle Guay,[§] Susan Nan,[§] Helen Yee,[§] Jason Crawford,[§] Gang Chen,[§] Trevor Wilson,[§] Bryon Carpenter,[§] David Gauthier,[§] Ron MacFarland,[§] Renee Mosi,[§] Veronique Bodart,[§] Rebecca Wong,[§] Simon Fricker,[‡] and Dominique Schols^{||}

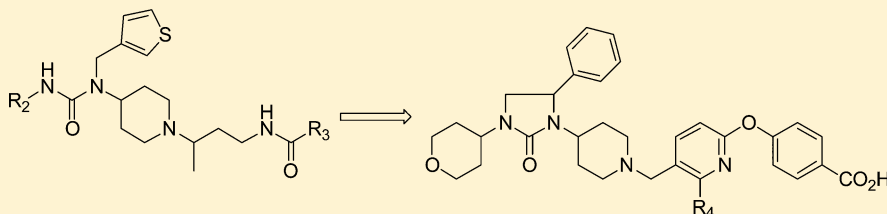
[†]LGCR Unit, Sanofi, 153 Second Avenue, Waltham, Massachusetts 02451, United States

[‡]Genzyme, a Sanofi company, 49 New York Avenue, Framingham, Massachusetts 01701, United States

[§]AnorMED Inc., 200-20353 64th Avenue, Langley, British Columbia V2Y 1N5, Canada

^{||}Rega Institute for Medical Research, Katholieke Universiteit Leuven, Minderbroedersstraat 10, Leuven B-3000, Belgium

Supporting Information



ABSTRACT: The redesign of the previously reported thiophene-3-yl-methyl urea series, as a result of potential cardiotoxicity, was successfully accomplished, resulting in the identification of a novel potent series of CCR5 antagonists containing the imidazolidinylpiperidinyl scaffold. The main redesign criteria were to reduce the number of rotatable bonds and to maintain an acceptable lipophilicity to mitigate hERG inhibition. The structure–activity relationship (SAR) that was developed was used to identify compounds with the best pharmacological profile to inhibit HIV-1. As a result, five advanced compounds, **6d**, **6e**, **6i**, **6h**, and **6k**, were further evaluated for receptor selectivity, antiviral activity against CCR5 using (R5) HIV-1 clinical isolates, and in vitro and in vivo safety. On the basis of these results, **6d** and **6h** were selected for further development.

INTRODUCTION

The recognition that the chemokine receptor CCR5 is required by HIV-1 as a coreceptor for cell entry^{1,2} together with the discovery that individuals lacking CCR5 because of a 32 bp deletion in the CCR5 gene are resistant to HIV-1 infection^{3,4} sparked a strong research interest to identify CCR5 small-molecule antagonists^{5–19} to treat HIV infection. This effort culminated in the marketing approval of the first-in-class chemokine receptor antagonist, maraviroc, in 2007.²⁰ Maraviroc represents a new class of therapeutic agents for the treatment of patients with HIV, which becomes very crucial in light of the viral resistance that develops over time.

Other small-molecule CCR5 inhibitors have failed in the clinic. For example, TAK-779 failed because of poor pharmacological and toxicological properties as well as a lack of oral bioavailability,⁷ SCH-C failed because of prolongations of the QT interval,⁷ vicriviroc failed because of viral rebound issues,²¹ and aplaviroc failed because of liver toxicity.²² Because of this attrition rate, there was a strong interest to develop

structurally diverse antagonists with improved pharmacokinetic, pharmacodynamic, and resistance profiles.

We have recently reported our efforts to design structurally unique compounds using SCH-C as our starting point. In a systematic approach, we first modified the piperidyl-amide group and then successfully discovered several new scaffolds for the benzoxime moiety^{23–25} (Figure 1). Mutation studies²⁶ investigated how these small molecules interact with CCR5, and, in agreement with the literature,^{27–35} all of the small-molecule antagonists tested so far share a common binding site in the transmembrane region beneath ECL 2. Because the binding site of these allosteric inhibitors is rather hydrophobic, we²⁵ and others^{36,37} encountered liabilities with hERG inhibition. In a recent publication,²⁵ we reported the identification of thiophene-3-yl-methyl ureas (**1**) as a novel class of CCR5 antagonists that exhibited potent inhibition of

Received: July 19, 2013

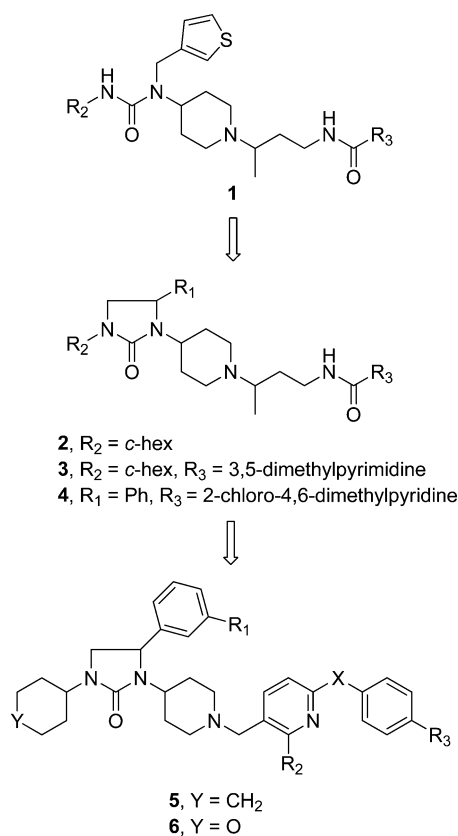


Figure 1. Structures of compounds 1–6.

R5 HIV-1 (BaL) replication in PBMC (Figure 1). Although these compounds had an acceptable hERG profile, they unexpectedly prolonged the APD in canine Purkinje fibers, suggesting a more complex mixed cardiac ion-channel effect. As a consequence, the development of these compounds was suspended.

In this Article, we describe our strategy in redesigning this chemotype as well as the subsequent SAR of the intermediate chemotypes (2–5) that resulted in the identification of compounds (6) that met the criteria for the pharmacological inhibition of HIV-1 but with no cardiac liability on the basis of the canine Purkinje fiber and hERG assays. The SAR was based on several in vitro assays. We utilized a gp120/CCR5 cell-fusion assay as a primary screen to select compounds for antiviral screening because the fusion data was found to be a reliable predictor of antiviral activity.²⁶ Antagonism of CCR5 was measured using the RANTES-induced Ca²⁺-flux inhibition and ¹²⁵I-RANTES competitive-binding assays, which were found to correlate well with the antiviral activity evaluated in PBMC utilizing the R5 HIV-1 clinical isolates and strains.³⁸

CHEMISTRY

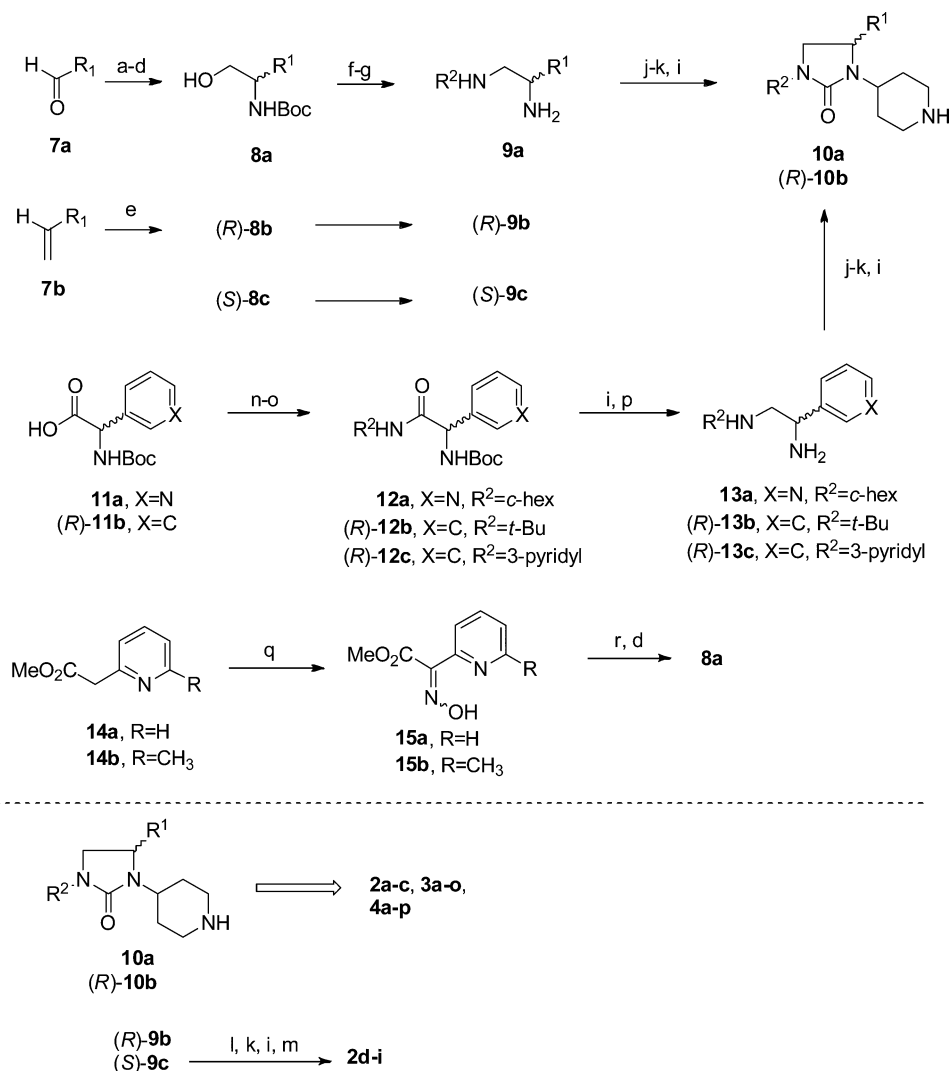
The general methodology utilized for the synthesis of the cyclic ureas 2–4 is shown in Scheme 1. The Strecker reaction was used to prepare the racemic α -amino nitrile precursors from commercially available aldehydes 7a, which were then readily reduced to the corresponding amino acids. Borane reduction of the acid to the alcohol followed by Boc protection of the amine afforded the corresponding racemic Boc-protected amino alcohols 8a. Mitsunobu reaction of alcohols 8a with *N*-(*Z*-amino)phthalimide gave the phthaloyl carbazates, which were cleaved with hydrazine to afford the corresponding Boc-

protected diamines. Reductive amination of the primary amine with commercially available ketones or aldehydes using NaBH(OAc)₃ or NaBH₄, respectively, followed by Boc deprotection using TFA afforded corresponding diamines 9a. A second reductive amination with *N*-(*t*-butoxycarbonyl)-piperidin-4-one installed the piperidine ring to give the disubstituted secondary amine that underwent Boc deprotection to afford cyclic ureas 10a. Alternatively, substituted vinyl precursors 7b (specifically, 3-vinylthiophene, 1-chloro-3-vinylbenzene, and 1-fluoro-3-vinylbenzene) were utilized for asymmetric aminohydroxylations³⁹ to afford the corresponding enantiomerically enriched amino alcohols (*R*)-8b (94% ee). Utilizing methodology that we previously reported,²³ compound 10a was readily converted to target compounds 2a–c and 3a–l (Tables 1 and 2). However, in the case of the single diastereomers (Table 1) and the compounds containing the (*R*)-phenyl group (Table 3), the starting materials were the commercially available (*R*)- and (*S*)-Boc-protected amino alcohols 8b and 8c, which were readily converted to diamines 9b and 9c. Reaction of (*R*)-9b and (*S*)-9c with (*R*) and (*S*)-*tert*-butyl (3-(4-oxopiperidin-1-yl)butyl)carbamate followed by treatment with triphosgene gave the corresponding cyclic ureas. Boc deprotection followed by standard amino acid coupling with 4,6-dimethylpyrimidine-5-carboxylic acid or 2-chloro-4,6-dimethylpyrimidine-5-carboxylic acid afforded single diastereomers 2d–i (Table 1). Following the conditions described above for the synthesis of the racemic compounds, intermediate 10b was used to synthesize target compounds 4a–c, 4e–l, and 4n–p (Table 3) as described.^{23–25}

In several examples, the starting material was the corresponding Boc-protected amino acid 11a and (*R*)-11b (Scheme 1). Activation of the acids using *iso*-butylchloroformate followed by reaction with a commercially available primary amine gave amides 12a–c. Boc deprotection followed by borane reduction of the amide afforded diamines 13a–c, which were converted to cyclic ureas 10a and 10b as described above. Ultimately, compounds 3m, 4d, and 4m (Tables 2 and 3) were synthesized using this procedure.^{23–25}

Pyridyl analogs 3n and 3o (Table 2) were prepared from the commercially available methyl esters 14a and 14b (Scheme 1). Installation of the oxime moiety, 15a and 15b, alpha to the ester using sodium nitrate in the presence of acetic acid followed by concomitant reduction of the ester and oxime groups to the hydroxy amine and Boc protection of the amine afforded compounds 8a, which were processed in a similar manner as mentioned above to yield compounds 3n and 3o.^{23–25}

The methodology used to prepare compounds 5 (Table 4) is shown in Scheme 2 using the advanced intermediate (*R*)-1-cyclohexyl-4-phenyl-3-(piperidin-4-yl)imidazolidin-2-one 10b. Reductive amination of 10b under standard conditions with a variety of substituted benzaldehydes afforded compounds 5a–p. The benzaldehyde precursors utilized to prepare 5a–f were readily synthesized by Suzuki cross coupling of 4-formyl benzene boronic acid with the appropriately substituted bromo heterocyclic ring to afford the coupled products in excellent yield. The precursor for 5g, 4-morpholinobenzaldehyde, was readily prepared using Buchwald cross-coupling chemistry. Similarly, the piperidine intermediate 1-(*o*-tolyl)piperidine-4-carbaldehyde precursor to 5i was prepared by Buchwald coupling of methyl piperidine-4-carboxylate and 1-bromo-2-methylbenzene. The intermediate 1*H*-benzo[*d*]imidazole-6-carbaldehyde used for 5h was simply prepared by TPAP

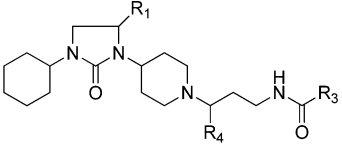
Scheme 1. Synthesis of Compounds 2–4^a

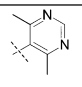
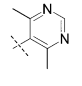
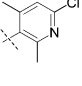
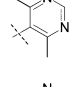
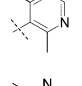
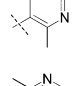
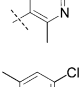
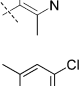
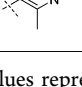
^aReagents: (a) NaCN, NH₄Cl, NH₄OH, MeOH, H₂O; (b) HCl 6 N, reflux; (c) BH₃·THF, reflux; (d) Boc₂O, Et₃N, THF; (e) NH₂Boc, *n*-PrOH, H₂O, *t*-BuOCl, (DHQD)₂PHAL, K₂OsO₂(OH)₄, 0 °C, 1 h, ee = 94%; (f) *N*-(*Z*-amino)phthalimide, DEAD, Ph₃P, THF; (g) hydrazine, EtOH; (h) R₂CO, NaBH(OAc)₃, CH₂Cl₂ or RCHO, NaBH₄, MeOH; (i) TFA, CH₂Cl₂, rt; (j) *N*-(*t*-butoxycarbonyl)piperidin-4-one, NaBH(OAc)₃, CH₂Cl₂; (k) triphosgene, pyridine, CH₂Cl₂; (l) (*R*)- or (*S*)-*tert*-butyl (3-(4-oxopiperidin-1-yl)butyl)carbamate, NaBH(OAc)₃, CH₂Cl₂; (m) 4,6-dimethylpyrimidine-5-carboxylic acid or 2-chloro-4,6-dimethylpyridine-5-carboxylic acid, EDCI, HOBT, NMM, THF/DMF; (n) *iso*-butyl chloroformate, NMM, THF; (o) R₂NH₂; (p) BH₃·THF, reflux; (q) NaNO₂, AcOH, H₂O; and (r) LAH, THF.

oxidation of the corresponding alcohol, which in turn was obtained from the ester. The precursor for **5j**, 4-formyl-*N*-methylbenzamide, was simply prepared by treatment of 4-carboxybenzaldehyde with methylamine hydrochloride. Finally, the phenoxy benzaldehydes used to prepare compounds **5k–p** and **6a** were synthesized as previously described.⁴⁰

Compounds **5q** and **5r** containing the bis-piperidinyl core were also prepared from advanced intermediate **10b** (Scheme 2). Following the procedure reported by Palani,⁴¹ intermediate **10b** was coupled with *N*-(*t*-butoxycarbonyl)piperidin-4-one in the presence of titanium(IV)isopropoxide followed by the addition of diethylaluminum cyanide. Methylation of the distal piperidyl ring was accomplished by treating the cyano group with an excess of methyl magnesium bromide. Boc deprotection followed by standard EDCI coupling with the corresponding aromatic acids^{23,24} afforded compounds **5q** and **5r**.

Scheme 3 summarizes the synthesis of compounds **6** (Table 5). The key step involved coupling of intermediate **10b** with the appropriately functionalized right-hand side intermediates **18a–f**. Intermediates **18a–b** were synthesized from the coupling of commercially available 2-bromo-5-methylpyridine **16** with corresponding phenol **17b** or thiol **17a**. Intermediate **18a** was used to prepare compounds **6b** and **6c**. For instance, treatment of chloride **18a** with Zn(CN)₂ in the presence of Pd(0) afforded the corresponding nitrile, which was ultimately used to liberate the carboxylic acid. The toluoyl group was used to install the electrophilic bromomethyl moiety using NBS, which then underwent *N*-alkylation with key intermediate **10b**. Subsequent base hydrolysis afforded the corresponding carboxylic acids **6b** or **6c**. However, intermediate acid **18b** was used to prepare compound **6i**, but the carboxylic acid group of **18b** was first protected as the corresponding methyl ester. As in the previous example, the toluoyl group was converted to the bromomethyl moiety, which underwent *N*-

Table 1. In Vitro Pharmacology of Compounds 2^a


Compd	R ₁	R ₄	R ₃	MW/ cLogP	CCR5 Fusion IC ₅₀ (nM)	CCR5 Ca Flux IC ₅₀ (nM)	RANTES ¹²⁵ I Binding IC ₅₀ (nM)	HIV-1 PBMC IC ₅₀ (nM)	PBMC CC ₅₀ (nM)
2a	3-thiophene	Me		539/3.5	39.0	85.0	44.4	nd	nd
2b	Ph	Me		533/3.8	65.7 (n=5)	20.7 (n=4)	77	nd	nd
2c	3-thiophene	Me		572/5.0	0.9 (n=4)	2.4 (n=2)	nd	30.0 (n=3)	>32100
2d	(R)-Ph	(R)-Me		533/3.8	27.6 (n=4)	13.6 (n=4)	19.8	>358.3 (n=2)	>35800
2e	(S)-Ph	(R)-Me		533/3.8	9039.0	>16000	nd	nd	nd
2f	(R)-Ph	(S)-Me		533/3.8	14.0 (n=2)	4.4 (n=3)	16.6	658.2 (n=2)	>35800
2g	(S)-Ph	(S)-Me		533/3.8	1839.0	1465.0	nd	nd	nd
2h	(R)-Ph	(R)-Me		566/5.4	1.2 (n=4)	1.5 (n=2)	13.6	49.2 (n=3)	33900
2i	(R)-Ph	(S)-Me		566/5.4	0.5 (n=4)	1.5 (n=2)	9.6	18.0 (n=3)	34300

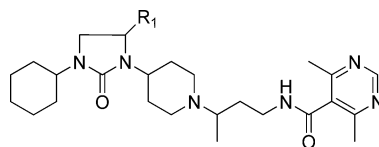
^aThe assays were performed in duplicate, and the values represent the mean with standard deviations of <30% of the mean. The bracketed values represent the number of experiments.

alkylation with **10b** followed by acid hydrolysis of the methyl ester to afford carboxylic acid **6i**. Compounds containing a 6-methylpyridyl substituted linker, **6d–g** and **6j–k**, were prepared using commercially available 6-bromo-2-methyl-3-carboxaldehyde **19a**. For example, coupling of **19a** with 4-hydroxybenzotrile **17c** afforded nitrile **18c**, which underwent reductive amination in the presence of NaBH(OAc)₃ with amine **10b** followed by acid hydrolysis to afford carboxylic acid **6k**. Compounds **6d–g** and **6j** were prepared in a similar manner as described above from phenol and thiol methyl esters **17d** and **17f**.⁴² Methyl amide **6l** was simply prepared from carboxylic acid **6d** via standard EDCI coupling. The same methodology was also used to prepare ethyl-containing analog **6h** starting from aldehyde **19b** and ester **17e**. Pyrimidine analog **6m** was prepared from 4-((5-vinylpyrimidin-2-yl)thio)benzoate **21**, which was obtained from the coupling of 5-bromo-2-chloropyrimidine **19** and 4-mercaptobenzoic acid **20** followed by the Pd(0)-catalyzed coupling of vinyltributylstannane to install the vinyl group. Oxidative cleavage of the vinyl group afforded the corresponding aldehyde, which was treated under reductive amination conditions with intermediate **10b** followed

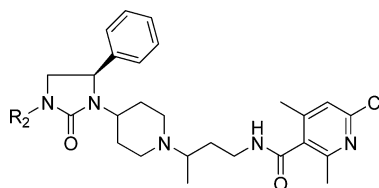
by base hydrolysis to afford carboxylic acid **6m**. To synthesize methyl pyrimidine analog **6n**, the intermediate 2-((4-bromophenyl)amino)-4-methylpyrimidine-5-carbaldehyde **24** was synthesized by the Pd(0)-catalyzed amination between ethyl 2-amino-4-methylpyrimidine-5-carboxylate **22** and dibromobenzene **23** followed by conversion of the ester to the aldehyde and the bromide to the nitrile. The coupling of aldehyde **24** with **10b** followed by nitrile hydrolysis afforded carboxylic acid **6n**.

RESULTS AND DISCUSSION

Rather than making incremental modifications to the existing chemotype, our goal was more ambitious, resulting in a complete redesign. Our main redesign criteria was to reduce the number of rotatable bonds on the basis of the retrospective analysis of large pharma compound collections that suggested that compound rigidity resulted in improved pharmacokinetic and pharmacological profiles.⁴³ The left-hand side urea of compound series **1** was an obvious area where the number of rotatable bonds could be reduced by synthesizing a cyclic urea.

Table 2. Comparative In Vitro Pharmacology of Compounds 3^a

compound	R ₁	MW/cLogP	CCRS fusion IC ₅₀ (nM)	CCRS Ca flux IC ₅₀ (nM)	RANTES ¹²⁵ I binding IC ₅₀ (nM)	HIV-1 PBMC IC ₅₀ (nM)	PBMC CC ₅₀ (nM)
2b	Ph	533/3.8	65.7	20.7 (n = 4)	77		
3a	2-Me-Ph	547/4.3	1702	322			
3b	2-F-Ph	551/3.9	342	91	155		
3c	2-Cl-Ph	567/4.5	3148	1526	195		
3d	3-Me-Ph	547/4.3	11.7 (n = 28)	6.0 (n = 27)	31		
3e	3-Br-Ph	612/4.7	10.4 (n = 4)	5.1 (n = 2)	22	347.9 (n = 3)	>32 699
3f	3-Cl-Ph	567/4.5	2.5 (n = 19)	5.8 (n = 18)	19.5	1777 (n = 3)	>34 742
3g	3-F-Ph	551/3.9	62.5	15.0 (n = 2)	25.9		
3h	3-CN-Ph	558/3.2	56.9 (n = 2)	32.2	34.8 (n = 2)		
3i	3-CO ₂ Me-Ph	591/3.6	346.5	157.6 (n = 3)	175.8		
3j	4-Br-Ph	612/4.7	3020	700.8			
3k	3,5-diMe-Ph	561/4.8	79.6	4.7 (n = 2)	36.5		
3l	3-F,5-Me-Ph	565/4.5	18.5 (n = 2)	7.1 (n = 3)	32.0 (n = 2)		
3m	3-Pyridyl	534/2.3	2938	832			
3n	2-Pyridyl	534/2.3	908.8 (n = 2)	300.7 (n = 2)			
3o	6-Me-2-Pyridyl	548/2.8	117.1	149.8			

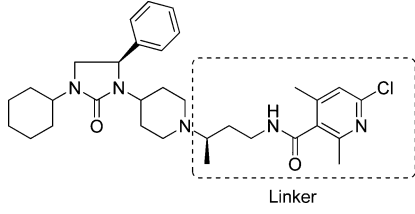
^aSee Table 1.Table 3. Comparative In Vitro Pharmacology of Compounds 4^a

compound	R ₂	MW/cLogP	CCRS fusion IC ₅₀ (nM)	CCRS Ca flux IC ₅₀ (nM)	RANTES ¹²⁵ I binding IC ₅₀ (nM)	HIV-1 PBMC IC ₅₀ (nM)	PBMC CC ₅₀ (nM)
4a	Et	512/3.8	56.6	24.7 (n = 2)			
4b	Pr	526/4.4	6.4 (n = 4)	7.5 (n = 2)	19.4		
4c	<i>i</i> -Pr	526/4.2	11.2 (n = 2)	5.3 (n = 2)			
4d	<i>t</i> -Bu	540/4.7	3.8 (n = 4)	3.6 (n = 2)		351.7 (n = 3)	>34 300
4e	<i>c</i> -Bu	538/4.3	1.7 (n = 4)	2.3 (n = 2)	19.5	549.9 (n = 3)	>33 500
4f	<i>c</i> -Pent	552/4.8	0.9 (n = 3)	0.9 (n = 2)			
4g	4-THP	568/3.0	8.6 (n = 4)	6.3 (n = 2)			
4h	4-THPCH ₂	582/3.7	1.1 (n = 2)	0.8 (n = 2)	14.6		
4i	<i>c</i> -HexCH ₂	580/6.1	0.9 (n = 3)	1.8 (n = 2)	7.7		
4j	Benzyl	574/5.2	1.2 (n = 4)	1.3 (n = 3)	9.0	12.3 (n = 5)	>34325
4k	2-PyridylCH ₂	575/3.7	5.9 (n = 2)	2.9 (n = 2)		1026.7	>34237
4l	3-(4-Me-Pyridyl)CH ₂	589/4.2	1.7 (n = 3)	1.2 (n = 2)	8.0		
4m	3-Pyridyl	561/3.9	9.3 (n = 2)	3.4 (n = 2)	52.4		
4n	4-PyridylCH ₂	575/3.7	1.0 (n = 3)	0.8 (n = 3)	5.7	12.2 (n = 3)	>32400
4o	HO ₂ C-4- <i>c</i> -Hex	610/1.6	56.0 (n = 2)	807.2			
4p	HO ₂ C-4-PhCH ₂	618/2.7	1.0 (n = 4)	3.6 (n = 2)	42.2 (n = 2)	14.3 (n = 4)	>32350

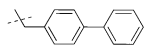
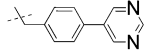
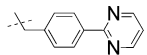
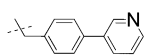
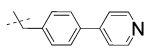
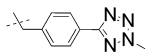
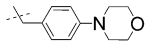
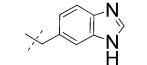
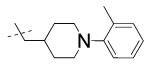
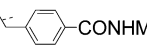
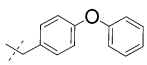
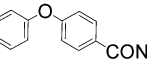
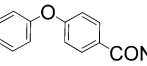
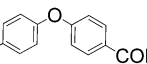
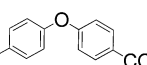
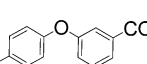
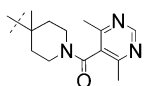
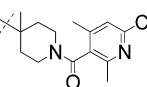
^aSee Table 1.

Given that an additional stereogenic center is generated, we sought to confirm that a phenyl substituent proximal to the urea nitrogen would have equivalent potency to the corresponding thiophene because the synthetic precursors to prepare the single enantiomers of the phenyl were commercially available. As shown in Table 1, there was a

marginal, <2-fold, loss in potency for phenyl compound 2b compared to thiophene compound 2a based on the CCR5-fusion and RANTES binding-inhibition assays. In addition, the SAR for compounds 1 also tracked with cyclic ureas 2. For example, using the optimized 2-chloro-4,6-dimethylpyridine amide group on the right-hand side, 2c resulted in an

Table 4. Comparative In Vitro Pharmacology of Compounds 5^a


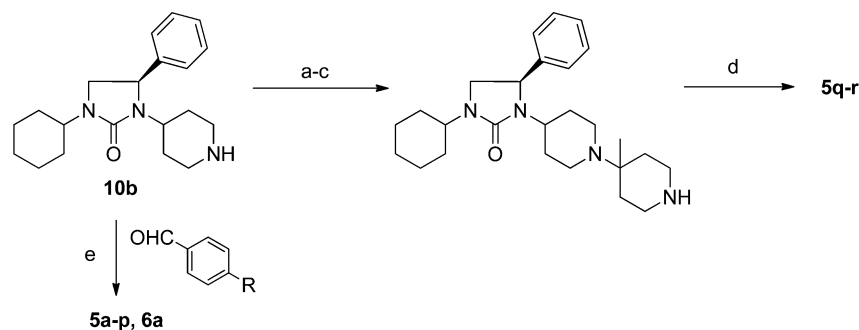
Linker

Compd	Linker	MW/ cLogP	Fusion IC ₅₀ (nM)	Ca Flux IC ₅₀ (nM)	RANTES ¹²⁵ I Binding IC ₅₀ (nM)	HIV-1 PBMC IC ₅₀ (nM)	PBMC CC ₅₀ (nM)
2j	Isobutyl chain	566/5.4	1.2 (n=4)	1.5 (n=2)	13.6	49.2 (n=3)	>33900
5a		494/7.1	435.9	12.4	41.8 (n=2)	nd	nd
5b		496/4.7	50.6 (n=80)	17.3 (n=78)	18.9	nd	nd
5c		496/4.9	2040 (n=4)	169.0 (n=3)	334.0 (n=2)	nd	nd
5d		495/5.6	214.0	17.9 (n=2)	43.7	nd	nd
5e		495/5.6	548.0 (n=2)	43.5	39.3	nd	nd
5f		500/4.8	279.5	43.7	nd	nd	nd
5g		503/4.7	336.2	15.2 (n=2)	nd	nd	nd
5h		458/4.6	199.7	91.0	50.7	nd	nd
5i		515/6.2	>1000	1595	nd	nd	nd
5j		475/3.9	62.7 (n=4)	15.8 (n=4)	85.1	nd	nd
5k		510/7.3	135.9	22.5 (n=2)	13.3	nd	nd
5l		567/6.0	44.7	11.6 (n=2)	9.6	3.2 (n=2)	14200
5m		581/5.8	57.0	7.5 (n=3)	15.5	24.2 (n=4)	14100
5n		553/5.8	28.8	6.9 (n=2)	18.0	39.6 (n=3)	14400
5o		554/4.8	13.0 (n=2)	6.4 (n=2)	38.9	34.3 (n=4)	>30000
5p		554/4.8	92.8 (n=2)	12.7 (n=2)	nd	nd	nd
5q		559/3.3	1.7 (n=4)	5.8 (n=2)	nd	107.1 (n=3)	>35800
5r		592/5.0	0.3 (n=4)	4.2 (n=2)	nd	<0.4 (n=3)	>35800

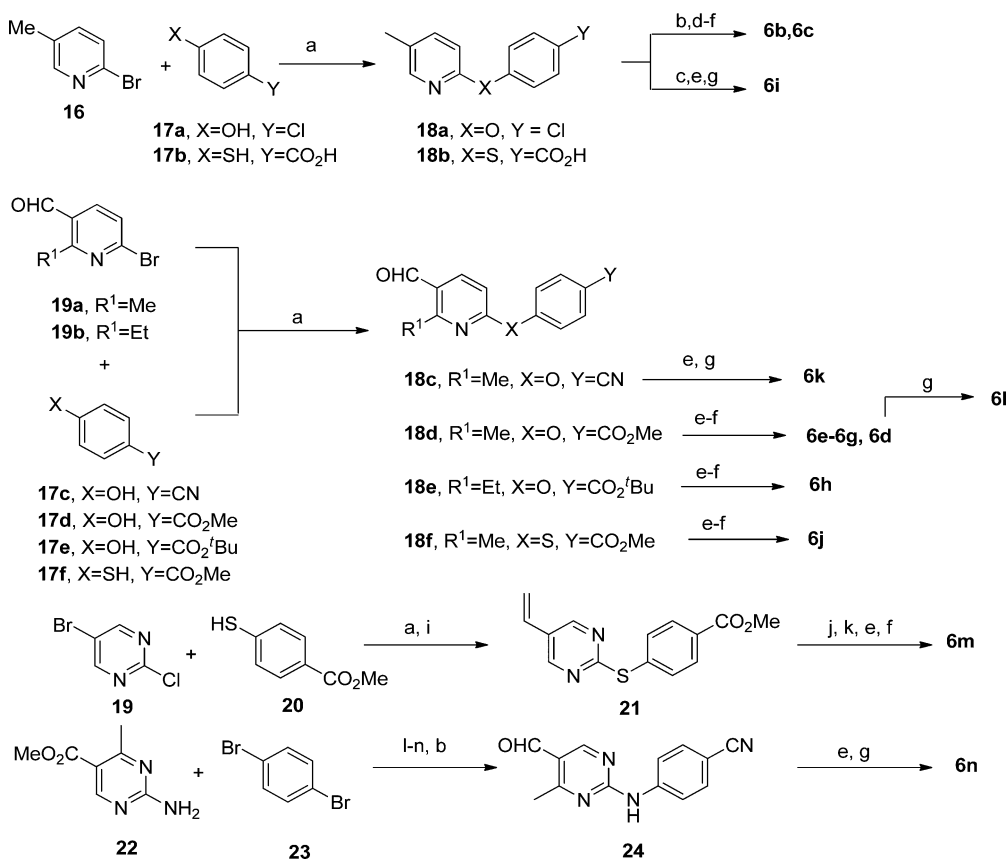
^aSee Table 1.

approximate 40-fold enhancement in potency compared to 2a, IC₅₀ of 0.9 versus 39.0 nM in the fusion-inhibition assay.

Moreover, we were encouraged that 2c exhibited antiviral activity in the PBMC HIV-1 assay at an IC₅₀ of 30 nM and was

Scheme 2. Synthesis of Compounds 5^a

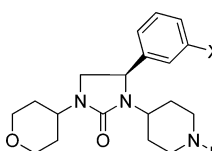
^aReagents: (a) 1-Boc-4-piperidone, Ti(OiPr)₄, CH₂Cl₂, rt, 48 h, then AlCNtEt₂, 20 h; (b) MeMgBr, THF, 0 °C to rt, 20 h; (c) TFA, CH₂Cl₂; (d) ArCO₂H, EDCl, HOBT, NMM, THF; and (e) RCHO, NaBH(OAc)₃, CH₂Cl₂, AcOH, rt.

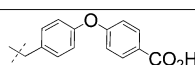
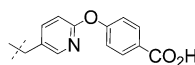

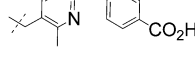
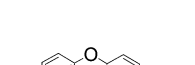
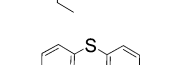
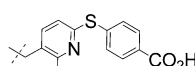
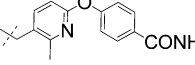
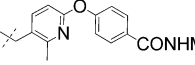
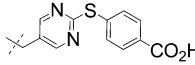
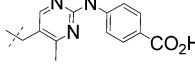
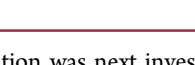
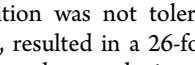
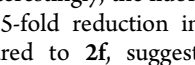
Scheme 3. Synthesis of Compounds 6^a

^aReagents: (a) K₂CO₃, DMF, 125–200 °C; (b) Zn(CN)₂, Zn dust, Pd₂(dba)₃, DPPF, DMAC, 145 °C; (c) H₂SO₄, MeOH, reflux, 15 h; (d) NBS, (PhCO)₂O₂, CCl₄, reflux, 4 h, then POH(OEt)₂, DIPEA, THF; (e) **10b**, CH₃CN, DIPEA or **10b**, NaBH(OAc)₃, AcOH, CH₂Cl₂, rt; (f) EtOH/10N NaOH, 60–90 °C, 5–18 h; (g) TFA, H₂SO₄ (4 drops); (h) MeNH₂, EDCl, hOBT, NMM, THF/DMF; (i) Pd(PPh₃)₂Cl₂, PPh₃, LiCl, DMF, CH₂CHSnBu₃, 100 °C, 18 h; (j) NMO, OsO₄, CH₂Cl₂, 18h; (k) NaIO₄, acetone, H₂O; (l) Pd₂(dba)₃, 4,5-bis(diphenylphosphine)-9,9-dimethylxanthane, *t*-BuOK, PhMe; (m) DIBAL-H, PhMe, –78 °C; and (n) MnO₂, CH₂Cl₂.

noncytotoxic to PBMCs, as measured by a CC₅₀ of >32 μM. On the basis of the comparable potency of the phenyl and thiophene groups, the corresponding four diastereoisomeric phenyl substituted ureas of **2b** were synthesized to rank the diastereoisomeric pair according to potency (Table 1). It was apparent that the preferred stereochemistry on the urea was (*R*), whereas the (*S*) configuration of the isobutyl chain was slightly preferred on the basis of the fusion-inhibition data. For example, the CCR5 fusion inhibition for the (*R,R*) pair **2d** was 27.6 nM, whereas for the (*S,R*) pair **2e** it was 9039 nM, a 330-

fold difference in IC₅₀. In contrast, the stereochemistry of the isobutyl chain had a moderate impact on fusion inhibition, as illustrated by the (*R,S*) pair **2f** where the fusion inhibition IC₅₀ was 14.0 nM, a 2-fold difference compared to compound **2d**. This trend was also evident using the optimum 2-chloro-4,6-dimethyl pyridine amide on the right-hand side, which agreed with the SAR for the thiophene-3-yl-methyl urea series **1**. For example, the (*R,S*) pair **2i** was antivorally more potent than the (*R,R*) pair **2h**, with an IC₅₀ of 18.0 versus 49.2 nM, which is consistent with the fusion-inhibition data of 0.5 versus 1.2 nM.

Table 5. Comparative In Vitro Pharmacology of Compounds 6^a


Compd	X	R	MW/ cLogP	CCR5 Fusion IC ₅₀ (nM)	Fold AGP fusion shift	HIV-1 PBMC IC ₅₀ (nM)	PBMC CC ₅₀ (nM)	Protein Binding %	hERG inhib. %	hERG IC ₅₀ (μM)
6a	H		556/ 2.4	15.7 (n=6)	1.0	190.1 (n=2)	>32500	90.2	1.9	>40
6b	H		557/ 0.9	6.6 (n=4)	0.7	39.7 (n=3)	>27300	91.8	2.9	nd
6c	Cl		591/ 1.6	1.3 (n=9)	1.1	36.5 (n=14)	>32200	94.5	20.8	nd
6d	H		571/ 1.3	1.4 (n=9)	1.1 (n=4)	24.1 (n=8)	>31300	93.3	4.9	>30
6e	Cl		605/ 2.1	0.6 (n=8)	1.2	0.6 (n=2)	>30500	95.7	8.4	9.9
6f	Me		585/ 1.8	1.1 (n=6)	0.9	0.8 (n=2)	>31500	95.7	19.2	nd
6g	F		589/ 1.5	1.5 (n=5)	0.6	91.8 (n=7)	>33900	94.8	2.2	nd
6h	H		585/ 1.9	0.7 (n=9)	1.0 (n=3)	34.7 (n=6)	>31900	97.6	26.5	>30
6i	H		573/ 1.7	0.9 (n=10)	0.9 (n=4)	4.0 (n=5)	>26200	91.4	2.1	>30
6j	H		587/ 2.2	0.4 (n=4)	1.0	0.1	>32000	94.3	17.7	nd
6k	H		569/ 2.2	1.1 (n=7)	1.5 (n=3)	7.9 (n=3)	>35100	89.4	10.0	18.0
6l	H		584/ 2.6	1.3 (n=4)	1.4	7.6 (n=2)	>30300	94.5	22.7	nd
6m	Cl		608/ 1.5	0.9 (n=5)	1.2	2.9 (n=3)	>30700	96.4	nd	nd
6n	Cl		605/ 1.8	0.9 (n=7)	1.8	36.1 (n=2)	>33100	89.0	6.0	nd

^aSee Table 1.

The effect of phenyl substitution was next investigated using pyrimidine amide **3** tested as a racemic mixture (Table 2). Substitution at the ortho position was not tolerated. Simple addition of a methyl group, **3a**, resulted in a 26-fold reduction in fusion inhibition compared to the unsubstituted analog **2f**, perhaps due to steric effects. Interestingly, the fluoro isostere **3b** resulted in an approximately 5-fold reduction in fusion and calcium-flux inhibition compared to **2f**, suggesting that an electronic effect was also in play. This was confirmed by the 2-chloro substituent **3c**, which was characterized by an approximately 50- and 70-fold reduction in inhibition for

fusion and calcium flux, respectively. In contrast, substitution at the meta position resulted in enhanced potency comparable to the SAR that we reported for an earlier aniline series.²³ For example, the 3-Me **3d** and 3-Br **3e** analogs resulted in an approximately 6-fold enhancement in potency based on the fusion assay, whereas the 3-Cl analog **3f** resulted in a 26-fold increase in fusion inhibition compared to **2f**, with an IC₅₀ of 2.5 versus 65.7 nM. More striking was the difference in fusion inhibition between the 2- and 3-Cl-substituted analogs, **3c** and **3f**, with IC₅₀ values of 3148 and 2.5 nM, a 1260-fold difference. Interestingly, the fluoro and cyano analogs, **3g** and **3h**, had no

effect on fusion or calcium-flux inhibition, whereas methyl ester **3i** resulted in a 5-fold loss in potency based on fusion and an 8-fold potency loss based on calcium-flux inhibition. A comparable loss in potency to the 2-substituted analogs was also observed for the 4-Br substituent **3j**, where the IC_{50} fusion inhibition was 3020 nM. Disubstitution of the phenyl at the 3- and 5-positions did not provide an additive effect, as shown by dimethyl analog **3k** and fluoro methyl analog **3l**. In an attempt to reduce the lipophilicity, substitution of the phenyl group by a pyridine group, either linked at the 2- or 3-position, compounds **3m** and **3n**, resulted in potency losses based on fusion inhibition. However, substitution of a methyl group at the 6-position (equivalent to the meta position of the phenyl), **3o**, regained some of the fusion potency.

Having determined that the optimum stereochemistry of the cyclic urea phenyl was (*R*), we kept this stereochemistry fixed to determine the optimum substitution at the urea nitrogen atom using the racemic isobutyl chain (the (*S*) isomer gave a moderate 2-fold enhancement in potency) attached to the optimal 2-chloro-4,6-dimethyl pyridine amide group, compounds **4** (Table 3). Although the cyclohexyl analog of compound **4** was not prepared, it can be inferred on the basis of the SAR from Table 1 that the activity would be comparable to the (*R,R*) isomer **2j** (e.g., comparison of **2a** to **2e**), which had a fusion inhibition IC_{50} of 1.2 nM. The effect of varying the size of the alkyl group from ethyl to cyclopentyl, **4a–f**, was investigated, and it appears that bulkier groups provide a potency comparable to the cyclohexyl analog. For example, the fusion inhibition for the *t*-Bu, *c*-Bu, and *c*-pent analogs **4d–f** were 3.8, 1.7, and 0.9 nM, which are comparable to the estimated IC_{50} of the cyclohexyl analog (1.2 nM). The addition of an oxygen atom, a potential hydrogen-bond acceptor, by the incorporation of a tetrahydropyran (THP) moiety, **4g**, resulted in an approximately 8-fold loss in fusion inhibition compared to the cyclohexyl analog. Interestingly, the potency was restored by adding a methylene linker, **4h**, between the THP group and the nitrogen urea. A similar level of fusion inhibition was observed for *c*-hex CH_2 **4i** and benzyl analogs **4j**, which correlated well with the anti-HIV-1 activity. For example, the IC_{50} value in the HIV-1 PBMC assay for compound **4j** was 12.3 nM. The incorporation of more hydrophilic pyridine groups, **4k–n**, was also investigated as a means of reducing the lipophilicity. It was found that the 4-pyridylmethylene analog **4n** had a comparable fusion inhibition to the cyclohexyl analog and, more importantly, had acceptable anti-HIV-1 potency of 12.2 nM. Previously, we have shown in the thiophene-3-yl-methyl urea series (**1**) that the addition of a carboxylic acid tethered to an appropriate sized linker, to pick up an ionic interaction with lysines located in the extracellular loop region of the receptor, mitigated hERG liability.⁴⁴ On the basis of the mutagenesis/molecular-modeling approach that we developed, we hypothesized that attaching the same carboxylic acid linker to cyclic urea **4** should generate potent compounds. This was indeed confirmed by the synthesis of compound **4p**, which had a fusion inhibition IC_{50} of 1.0 nM and an anti-HIV-1 activity of 14.3 nM. Similar to what had previously been reported,⁴⁴ the length of the linker chain is important, as highlighted by compound **4o** where the fusion inhibition was approximately 50-fold lower compared to **4p**.

Although the antiviral potency of compounds **4n** and **4p** met the criteria for the pharmacological inhibition of R5 HIV-1 replication, the oral bioavailability based on rat and dog pharmacokinetics was poor (data not shown). As a

consequence, we sought to enhance the pharmacokinetic properties by further reducing the number of rotatable bonds. Replacements of the entire isobutyl linker were investigated with the initial focus on maintaining potency (Table 4). Synthesis of biphenyl linker **5a** resulted in a substantial 360-fold loss in potency based on fusion inhibition but only a 3–8-fold loss in potency based on CCR5 Ca^{2+} -flux inhibition and ^{125}I -RANTES binding inhibition compared to compound **2j**. Adding hydrophilicity to the molecule by including a pyrimidine ring at the terminus **5b** improved the fusion inhibition 9-fold to an IC_{50} of 50.6 nM compared to **5a**. Interestingly, 2-substituted pyrimidine **5c** was substantially less potent than **5a** based on fusion, Ca^{2+} flux, and ^{125}I -RANTES binding inhibition, indicating that perhaps an H-bond acceptor at the terminal position was important for CCR5 inhibition. Several compounds containing H-bond acceptor moieties were synthesized, such as pyridine **5d–e**, tetrazole **5f**, morpholine **5g**, and benzimidazole **5h**. However, none of these compounds resulted in an improvement in fusion or Ca^{2+} -flux inhibition compared to **5b**. The incorporation of a phenyl piperidine, **5i**, resulted in a complete loss in activity. However, we were encouraged by the addition of a secondary amide, **5j**. For instance, the activity was restored to that of **5b** where the fusion IC_{50} was 62.7 versus 50.6 nM, and the Ca^{2+} -flux inhibition IC_{50} was 15.8 versus 17.3 nM. In addition, replacement of the linker with a phenoxy phenyl group, **5k**, also resulted in encouraging activity. On the basis of our modeling/mutagenesis studies,⁴⁴ we determined that extension of the chain containing a hydrophilic group would pick up additional interactions in the extracellular region. As a consequence, phenoxy amide **5l** was synthesized, and the inhibition profile showed marginal enhancements in the CCR5 Ca^{2+} -flux inhibition and ^{125}I -RANTES binding-inhibition assays, but more importantly the anti-HIV-1 activity was 3.2 nM. Primary amide **5n** and tertiary amide **5m** were also synthesized. These compounds had comparable fusion inhibition compared to **5l** but were approximately 2-fold less potent based on ^{125}I -RANTES binding inhibition, which resulted in an approximately 10-fold loss in anti-HIV-1 potency. In an effort to reduce the lipophilicity and to mitigate potential hERG liabilities, the *m*- and *p*-carboxylic acids, **5p** and **5o**, were synthesized. *p*-Substituted acid **5o** was 7-fold more potent based on fusion inhibition than the *m*-carboxylic acid, **5p**, and the anti-HIV-1 activity was 34.3 nM.

Given that the imidazolidinyl moiety is a novel chemotype in the context of CCR5 inhibitors as well as modeling studies that suggested that attachment of the (4,6-dimethylpyrimidin-5-yl)(piperidin-1-yl)methanone moiety of vicriviroc would be tolerated, we synthesized compound **5q**, which resulted in a fusion inhibition of 1.7 nM and anti-HIV-1 activity of 107.1 nM. On the basis of this encouraging result, we replaced the pyrimidine amide with our optimized 2-chloro-4,6-dimethyl amide, resulting in a very potent compound, **5r**; >250-fold enhancement in anti-HIV-1 activity compared to **5q** (IC_{50} of <0.4 nM).⁴⁵

Having demonstrated that suitable replacements for the isobutyl linker could be achieved without compromising antiviral potency, our goal shifted to reducing lipophilicity to mitigate off-target effects (Table 5). We demonstrated that incorporation of a tetrahydropyran group on the left-hand side rather than a cyclohexyl group lowered the cLogP by almost 2.5 orders of magnitude, **4g** (Table 3, cLogP 3.0) versus **2j** (Table 1, cLogP 5.4). In addition, we showed that the potency could

Table 6. Selected In Vitro Properties for Compounds 6d, 6e, 6h, 6i, and 6k

compound	HIV-1 PBMC IC ₅₀ (nM)	HIV-1 PBMC AGP fold change ^a	HIV-1 PBMC IC ₉₀ (nM)	HIV-1 PBMC AGP fold change ^a	Pe value (cm/sec × 10 ⁻⁶)	IC ₅₀ values in CYP assays (μM) ^b	microsomal stability (%)		
							rat	dog	human
6d	24.1 (n = 8)	5.1	222.0 (n = 8)	0.8	7.8	>40	16	6	8
6e	0.6 (n = 2)	0.3	3.9 (n = 5)	0.7	nd	>100	38	13	18
6h	34.7 (n = 6)	1.4	279.4 (n = 8)	0.7	12.2	>73	36	35	4
6i	4.0 (n = 5)	1.3	43.2 (n = 5)	1.0	11.7	>60	49	6	9
6k	7.9 (n = 3)	0.3	112.5 (n = 3)	0.3	12.0	>26	71	22	44

^aRatio of HIV-1 PBMC IC₉₀ or IC₅₀ with and without AGP. ^bThe lower limit in any of the CYP assays is shown: CYP450 1A2, 2B6, 2C8, 2C9, 2C19, 2D6, and 3A4.

Table 7. Chemokine Receptor Selectivity Profiles for Compounds 6d, 6e, 6h, 6i, and 6k

compound	CCR1 inhibition (%) ^a	CCR2b inhibition (%) ^a	CCR4 IC ₅₀ (nM) ^b	CCR7 inhibition (%) ^a	CXCR3 inhibition (%) ^a	CXCR4 inhibition (%) ^a
6d	91.4 (n = 2)	89.2 (n = 2)	566.2	83.8 (n = 2)	89.5 (n = 2)	103.1 (n = 2)
6e	84.9 (n = 2)	87.2 (n = 2)	283.4 (n = 2)	80.1 (n = 2)	91.0% (n = 2)	90.4 (n = 2)
6h	103.4 (n = 2)	88.7 (n = 2)	73.4% ^a (n = 2)	93.6 (n = 2)	99.7 (n = 2)	93.8 (n = 2)
6i	73.8 (n = 2)	95.6 (n = 2)	3723 (n = 1)	90.1 (n = 2)	66.7 (n = 2)	88.6 (n = 2)
6k	81.9 (n = 2)	97.3 (n = 2)	22.5% ^a (n = 2)	75.5 (n = 2)	67.8 (n = 2)	84.7 (n = 2)

^aPercent inhibition of receptor-mediated calcium flux with 5 μM compound. ^bInhibition results for receptor-mediated calcium flux are expressed as IC₅₀ (nM) if not otherwise specified.

be enhanced by substitution of the phenyl ring with a 3-Cl or 3-Me substituent on the basis of the SAR from Table 2. Aside from antiviral potency, the properties that were used to prioritize these analogs was the effect of AGP on fusion inhibition (AGP fusion shift) because HIV-infected patients exhibit elevated levels of AGP that can reduce the level of free drug, particularly of a basic compound, human plasma protein binding, and hERG inhibition based on the percent inhibition and/or IC₅₀.

As predicted, the cLogP of compound 6a containing a tetrahydropyran group was lower when compared to cyclohexyl analog 5o, 2.4 versus 4.8. Although the fusion inhibition of 6a was comparable to 5o, the anti-HIV potency was approximately 5-fold lower. However, the other properties were acceptable; for example, the hERG IC₅₀ was >40 μM, the fold AGP fusion shift was 1.0, and the human plasma protein binding was 90.2%. To reduce the lipophilicity further, the phenyl linker was replaced with a pyridine ring, 6b, reducing the cLogP from 2.4 to 0.9. This resulted in a 2-fold increase in fusion inhibition, a 5-fold increase in anti-HIV-1 potency (IC₅₀ of 39.7 nM), and in comparison to 6a the other properties remained essentially unchanged. In an attempt to increase the potency further, 3-Cl substituent 6c was synthesized, and although the fusion inhibition increased 5-fold the anti-HIV-1 activity remained unchanged at an IC₅₀ of 36.5 nM. On the basis of the SAR earlier developed for the isobutyl linker,²³ we were curious to determine if the addition of a methyl group to the pyridine ring would enhance the potency. A comparison of des-methyl compound 6b with the 6-methylpyridine compound 6d provided approximately a 5-fold increase in fusion inhibition but a comparable anti-HIV-1 activity, 39.7 versus 24.1 nM, respectively. In addition, the hERG inhibition was 4.9%, corresponding to an IC₅₀ of >30 μM. Interestingly, when the 6-methylpyridine moiety was combined with the 3-Cl-, 6e, 3-Me-, 6f, or 6-F-, 6g, substituted phenyl groups, the fusion inhibition remained unchanged at approximately 1 nM, but the anti-HIV-1 activity was significantly enhanced for 6e and 6f. For example, in comparison to 6c, the 3-Cl analog 6e was 60-

fold more potent with an IC₅₀ of 0.6 nM. However, it was surprising to observe that the anti-HIV-1 activity of the 6-F derivative, 6g, was lower at 91.8 nM. The addition of an ethyl group, 6h, resulted in a comparable property profile compared to 6d. Replacing the ether linkage with a thioether, 6i, also provided an enhancement in anti-HIV-1 activity compared to the corresponding ether analog 6d, with an IC₅₀ of 4.0 versus 24.1 nM. Moreover, the other critical parameters remained unchanged. The addition of a 6-methylpyridine moiety, 6j, to the linker provided a 40-fold enhancement in antiviral activity similar to what was observed in the ether examples. Substitution of the carboxylic acid for an amide, 6k and 6l, provided an approximately 3-fold increase in anti-HIV-1 potency. However, comparison of 6k to 6d showed that the hERG inhibition was higher, with an IC₅₀ of 18 versus >30 μM for 6d, and compared to 6l the hERG inhibition was 22.7 versus 4.9% for 6d. In addition, generally, the amide analogs, 6k and 6l, were more highly metabolized on the basis of their in vitro metabolic stability in human and rat liver microsomes, and this was correlated with low oral bioavailability in rat (data not shown). Importantly, although 6k and 6l had very comparable profiles, 6k was chosen for further evaluation because plasma protein binding was lower compared to 6l (89.4 vs 94.5%), as shown in Table 5. To increase polarity further, a series of pyrimidine analogs⁴⁰ were synthesized, represented by 6m and 6n, as shown in Table 5. The increased polarity of the pyrimidine group compensated for the additional 3-chloro group, 6m, and methyl group, 6n. For example, the cLogP of 1.5 of compound 6m remained virtually unchanged compared to the parent compound 6i. The fusion inhibition, anti-HIV-1 activity, and human plasma protein binding did not change significantly. The replacement of the thioether linkage by an aniline group improved the human plasma protein binding to 89%. Although this modification was tolerated in the fusion inhibition assay, the anti-HIV-1 activity dropped more than 10-fold.

In Table 6, the ADME in vitro properties of five lead compounds, 6d, 6e, 6h, 6i, and 6k, are shown in addition to the

Table 8. Dog Purkinje Fiber Data and hERG Data for Compounds **6d**, **6e**, **6i**, and **6k**^a

compound ^b	BCL (s)	$\Delta\%$		$\Delta_m V$		V_{max} ($\Delta\%$)	hERG IC ₅₀ (μM)
		APD ₆₀	APD ₉₀	RMP	APA		
6d	2	-2.9 \pm 2.5	-2.8 \pm 2.1	0.1 \pm 1.4	2.6 \pm 2.7	11.0 \pm 9.7	>30
	1	-4.0 \pm 2.8	-3.8 \pm 2.4	0.4 \pm 1.0	2.4 \pm 2.1	8.4 \pm 6.3	
	0.5	-4.0 \pm 2.6	-3.5 \pm 2.1	1.2 \pm 1.2	0.8 \pm 2.1	11.8 \pm 5.1	
6e	2	-10.5 \pm 7.2	-7.8 \pm 5.3	0.7 \pm 0.4	-4.4 \pm 4.0	-10.5 \pm 14.7	9.9
	1	-8.2 \pm 7.7	-6.4 \pm 5.8	0.1 \pm 0.2	-3.4 \pm 3.4	-11.2 \pm 11.2	
	0.5	-4.9 \pm 6.0	-3.4 \pm 4.2	-0.1 \pm 0.4	-1.8 \pm 3.6	5.4 \pm 16.2	
6i	2	-6.1* \pm 1.7	-7.0* \pm 0.5	-2.2 \pm 0.8	4.1 \pm 1.9	10.2 \pm 4.5	>30
	1	-4.6* \pm 1.5	-6.2* \pm 0.8	0.4 \pm 1.7	-0.9 \pm 3.3	4.5 \pm 2.3	
	0.5	-4.2* \pm 2.0	-6.2* \pm 1.3	0.7 \pm 1.9	-1.5 \pm 2.3	2.2 \pm 2.7	
6k	2	1.2 \pm 3.2	1.0 \pm 2.1	-1.6 \pm 1.3	-3.4 \pm 4.7	-0.8 \pm 8.3	18.0
	1	-1.7 \pm 5.4	1.8 \pm 1.7	-0.5 \pm 3.3	7.8 \pm 14.3	-15.6 \pm 12.9	
	0.5	-6.0 \pm 6.2	-0.3 \pm 1.1	-0.5 \pm 2.8	7.9 \pm 14.0	-16.7 \pm 9.9	

^aAction-potential parameters are reported as means \pm SDs, percent change ($\Delta\%$), increase (+), or decrease (-) in test-compound-exposed Purkinje fibers over those measured in time-matched vehicle control. APD₆₀ and APD₉₀ are the action-potential durations at 60 and 90% repolarization, respectively; RMP is the resting membrane potential; APA is the action-potential amplitude; V_{max} is the maximum velocity of phase 0 depolarization; and BCL is the basic cycle length. ^bThe compounds were tested at 10 μM . * $P < 0.05$.

Table 9. Anti-HIV-1 Activity Profile of Compounds **6d**, **6e**, **6h**, **6i**, and **6k** and Maraviroc^a

clade	6d		6e		6h		6i		6k		maraviroc	
	IC ₅₀	IC ₉₀	IC ₅₀	IC ₉₀	IC ₅₀	IC ₉₀	IC ₅₀	IC ₉₀	IC ₅₀	IC ₉₀	IC ₅₀	IC ₉₀
UG273 clade A	8.0	93.8	27.9	86.2	68.0	200	78.0	522.6	61.9	546.1	7.1	22.7
U52 clade B	0.23	3.8	0.5	12.7	1.4	5.7	0.6	4.7	<0.1	0.8	0.3	2.6
ETH2220 clade C	14.7	77.8	2.8	80.1	173.9	>1000	>1000	>1000	>1000	>1000	50.4	101.2
ID12 clade E	9.4	30.0	7.0	21.5	13.6	40	4.0	56.9	4.0	56.9	14.6	57.5
BZ163 clade G	15.0	78.9	33.2	89.8	6.5	105.3	16.2	463.0	16.2	463.0	14.8	71.8
I-2478B clade O	2.2	8.2	31.2	81.9	0.4	1.2	<0.1	0.1	<0.1	0.1	6.4	16
SF162 clade B	17.6	83.4	10.6	29.2	nd	nd	nd	nd	nd	nd	18.6	105.3
Ada clade B	6.0	26.5	2.0	6.1	1.4	5.6	0.6	15.6	<0.3	12.9	<0.3	33.6
CI#15 clade B	2.5	16.1	35.8	82.1	nd	nd	nd	nd	nd	nd	1.4	8.3
CI#19 clade B	0.7	19.5	5.4	16	nd	nd	nd	nd	nd	nd	1.3	11.9
BaL clade B	9.8	84.6	23.4	78.2	nd	nd	nd	nd	nd	nd	13.9	89.1

^aAll IC₅₀ and IC₉₀ values are reported in nM and were evaluated in PBMCs.

antiviral activity expressed both in IC₅₀ and IC₉₀. Importantly and similar to what was observed with fusion inhibition, the anti-HIV-1 activity is not significantly affected by AGP (HIV-1 PBMC IC₅₀ or IC₉₀ fold change), indicating that the probability of AGP reducing the in vivo efficacy of these compounds is low. Even though several of these compounds are zwitterionic, they had good cell permeability, as measured by the PAMPA assay, and more importantly they had good exposure when dosed orally in dog (vide infra). The propensity for drug–drug interactions was very low on the basis of cytochrome P450 IC₅₀ inhibition ranging from >26 to >100 μM for seven primary drug-metabolizing isozymes. The microsomal stability varied across species, but our optimization efforts focused on human, and it was evident that stability in general was the best in human followed by dog. Although the in vitro microsomal stability in rat was poor, this observation did not correlate well with the observed in vivo stability (vide infra).

Compounds **6d**, **6e**, **6h**, **6i**, and **6k** were tested against a panel of chemokine receptors for selectivity. The data in Table 7 shows that these compounds demonstrated little or no inhibition of the closely related chemokine receptors CCR1, CCR2b, CCR7, CXCR3, and CXCR4, with IC₅₀ values of at least >5 μM (the maximum concentration tested) compared to the IC₅₀ values against CCR5, which are in the range of 0.6–1.4 nM. Limited inhibition of CCR4 was observed for **6d**, **6e**, **6i**,

and **6k**, with the lowest IC₅₀ value of 283 nM for **6e**, which is approximately a 470-fold selectivity for CCR5. The IC₅₀ for **6h** was >5 μM . The potential pharmacological or toxicological effect of this limited inhibition of CCR4 is unknown, although it can be predicted that this will not be of toxicological significance because CCR4 knockout mice develop normally and are viable.^{46–48}

The four compounds, **6d**, **6e**, **6i**, and **6k**, were evaluated in the canine Purkinje fiber assay to understand the risk for drug-induced arrhythmias further (Table 8). There was an insignificant prolongation of the action-potential duration (APD) when all of the compounds were tested at 10 μM using the three standard stimulation frequencies, which is consistent with a lack of effect on the hERG potassium channel. For example, the four compounds inhibited hERG at IC₅₀ values of 9.9 to >30 μM , and the percent change in APD₆₀ at a basic cycle length (BCL) of 2 s was insignificant in the range of 3–10%. There was also no occurrence of early after depolarizations (EADs), and because the prolongation of APD₆₀ and APD₉₀ was similar at every stimulation cycle, there was no evidence of triangulation of the action potential. The lack of an effect on the resting membrane potential (RMP) or the rate of depolarization (V_{max}) also suggests that sodium channels are not inhibited at the concentrations tested. Hence,

Table 10. Pharmacokinetics of Compounds 6d, 6e, 6h, 6i, and 6k in Dog^a

compound	C _{max} (μM)	AUC _{0→inf} (h μM)	CL (mL/min/kg)	V (L/kg)	t _{1/2} (h)	F (%)
6d	14.4	37.96	0.30	1.23	2.83	91.4
6e	9.31	18.14	0.52	5.18	6.97	75.5
6h	38.6	128.55	0.11	0.49	3.00	117.2
6i	0.91	0.75	2.05	7.91	2.67	12.3
6k	11.3	47.45	0.22	1.16	3.61	85.5

^aClearance (CL), volume of distribution (V), and half-life (t_{1/2}) were calculated following a 5 μmol/kg iv dose. C_{max}, AUC, and oral bioavailability (F) were calculated following solution doses of 12.5 μmol/kg.

on the basis of these results, the risk for drug-induced arrhythmias is low.

A limited clade analysis, against six of the most common clades, was also undertaken. Included in the analysis were six strains of clade B, dominant in Europe, the Americas, and parts of Asia. The IC₅₀ and IC₉₀ of the five lead compounds were measured using maraviroc as a comparator (Table 9). Comparison of the five compounds against maraviroc using clade B (US2) showed that all compounds were at least comparable to or superior to maraviroc regarding their antiviral potency. This observation also held up against the other five clades. Interestingly, the relative potency of the five compounds reflected what was observed in the internal screening using PBMCs. Clearly, the excellent potency of these compounds across a diverse set of clades was an important criteria that was fulfilled.

Pharmacokinetic parameters were important in choosing compounds for further evaluation. However, because we observed a poor in vivo/in vitro correlation regarding their stability in rat, we conducted only oral rat exposure (data not shown) and used this data as a prescreen for a more complete pharmacokinetic analysis in dogs. Table 10 shows the pharmacokinetic data for compounds 6d, 6e, 6h, 6i, and 6k in dog, all of which had acceptable exposure in rat. With the exception of compound 6i, the compounds exhibited low clearance and reasonable exposure, resulting in good oral bioavailability. The volume of distribution was low for compounds 6d, 6h, and 6k, and all of the compounds exhibited reasonable half-lives.

The in vivo safety of the five lead compounds was evaluated in a 7-day repeat-dose toxicology study in rat at three dose levels (low, mid, and high). We were pleased to observe that all of the compounds were well tolerated across all doses, resulting in a NOAEL equivalent to the high dose (150–800 mg/kg). In addition, a comparison of the exposures at days 1 and 7 showed no evidence of accumulation.

Because the five lead compounds containing the novel chemotype, imidazolidinylpiperidinylbenzoic acid, were well tolerated in the rat safety study and ex vivo safety cardiotoxicity studies (Purkinje Fiber assay and hERG), other criteria were considered to prioritize the compounds for further development. An important factor taken into consideration was the off-target risk associated with inhibiting other receptors. For example, compounds 6e and 6k showed cross reactivity against CCR4 at 284 nM and 22% inhibition, respectively (Table 7). In addition, on the basis of the lower human microsomal stability of 6e and 6k, these compounds were not considered for further evaluation. Of the three remaining compounds, because 6i exhibited poor dog PK and the next safety study was a 7-day repeat-dose toxicology study in dog, compounds 6d and 6h were prioritized for further development.

CONCLUSIONS

The successful redesign of an earlier reported series, as a result of potential cardiotoxicity, was accomplished by focusing on reducing the number of rotatable bonds as well as maintaining an acceptable lipophilicity to mitigate hERG inhibition. As a result, a potent series of CCR5 antagonists containing the novel imidazolidinylpiperidinyl scaffold were identified that demonstrate significantly reduced cardiac liability based on hERG and canine Purkinje fiber experiments. Five compounds from this series, 6d, 6e, 6i, 6h, and 6k, were further evaluated for receptor selectivity, antiviral activity against CCR5 using (R5) HIV-1 clinical isolates, and in vitro and in vivo safety. All five compounds showed comparable or superior potency compared to maraviroc in a HIV-1 clade analysis study and were well tolerated in 7-day repeat toxicology studies in rat. However, on the basis of differences in chemokine receptor selectivity, metabolic stability, and pharmacokinetics, 6d and 6h were identified as candidates for further development.

EXPERIMENTAL SECTION

General Information. Unless otherwise noted, most of the reagents and solvents were purchased at the highest commercial quality and used without further purification. All reactions involving air- and/or moisture-sensitive reagents were performed under a nitrogen or argon atmosphere. Silica gel chromatography was performed using glass columns packed with silica gel 60 (40–63 μM, VWR International). ¹H and ¹³C NMR spectra were recorded at 300 and 75 MHz, respectively, on a Bruker Avance 300 spectrometer, with shifts referenced to the residual proton shift of the internal deuterated solvent. Electrospray mass spectra were recorded on a Bruker-HP Esquire-LC ion-trap mass spectrometer. Microanalyses for C, H, N, and halogen were performed by Atlantic Microlab, Inc. (Norcross, GA) and were within 0.4% of theoretical values. Purity was determined by reversed-phase HPLC and was ≥95% for all compounds tested.

General Procedure A. To a stirred solution of the amine (1 equiv) in CH₂Cl₂ (concentration ~0.2M) at room temperature were added the carbonyl compound (1 to 2 equivs), glacial AcOH (0–2 equivs), and NaBH(OAc)₃ (1.5–3.0 equivs), and the resultant solution was stirred at room temperature. In a standard workup, the reaction mixture was poured into either saturated aqueous NaHCO₃ or 1 N NaOH. The phases were separated, and the aqueous phase was extracted with CH₂Cl₂. The combined organic extracts were dried (Na₂SO₄ or MgSO₄), filtered, and concentrated under reduced pressure. The crude material was purified by flash column chromatography on silica gel or by recrystallization.

General Procedure B. The BOC-protected amine was dissolved in CH₂Cl₂ (~4 mL/mmol), and trifluoroacetic acid (TFA) (~2 mL/mmol) was added. The mixture was stirred at room temperature for 0.5–5 h. In a standard workup, the mixture was neutralized with saturated aqueous NaHCO₃ or 1 N NaOH, and the aqueous phase was extracted with CH₂Cl₂. The combined extracts were dried (Na₂SO₄ or MgSO₄), filtered, and concentrated under reduced pressure. The crude material was used in the next reaction as is or was purified by flash column chromatography on silica gel.

General Procedure C. The ester (1.0 equiv) was dissolved in a 1:1 MeOH/2 N NaOH solution. The reaction was stirred at 50 °C for 5–18 h. The mixture was concentrated under reduced pressure, and water was added. The pH of the solution was adjusted to ~4 to 5 with a 6 N HCl solution. The aqueous solution was then extracted with CH₂Cl₂ or a mixture of CH₂Cl₂/MeOH (9:1). The combined organic extracts were dried (Na₂SO₄ or MgSO₄), filtered, and concentrated under reduced pressure. The crude material was purified by flash column chromatography on silica gel or by recrystallization.

General Procedure D. The secondary amine (1.1 equivs) was dissolved in CH₃CN (concentration ~0.1 M). DIPEA (1.5 equivs) followed by a halide reagent (1.0 equiv) were added. The reaction was heated at 50–75 °C for 18 h. The mixture was concentrated under reduced pressure, and CH₂Cl₂ and saturated aqueous NaHCO₃ were added. The aqueous layer was extracted with CH₂Cl₂, and the combined organic extracts were dried (Na₂SO₄ or MgSO₄), filtered, and concentrated under reduced pressure. The crude material was purified by flash column chromatography or by radial chromatography on silica gel.

(R)-4-((6-Methyl-5-((4-(2-oxo-5-phenyl-3-(tetrahydro-2H-pyran-4-yl)imidazolidin-1-yl)piperidin-1-yl)methyl)pyridin-2-yl)oxy)benzoic Acid (6d). A mixture of 6-bromo-2-methylpyridine-3-carboxaldehyde (4.00 g, 20.0 mmol), 4-hydroxybenzoic acid methyl ester (3.80 g, 25.0 mmol), and K₂CO₃ (1.73 g, 12.5 mmol) in DMF (30 mL) was heated at 130 °C for 2 h. The mixture was cooled to room temperature, and DMF was removed. Aqueous workup and purification by flash chromatography on silica gel (CH₃OH/CH₂Cl₂, 1:50 in v/v) afforded methyl 4-((5-formyl-6-methylpyridin-2-yl)oxy)benzoate as a white solid (3.20 g, 59%). ¹H NMR (300 MHz, CDCl₃) δ 2.72 (s, 3H), 3.93 (s, 3H), 6.86 (d, 1H, J = 8.4 Hz), 7.20–7.25 (m, 2H), 8.08–8.15 (m, 3H), 10.25 (s, 1H). Following general procedure A, (R)-1-cyclohexyl-4-phenyl-3-(piperidin-4-yl)imidazolidin-2-one **10b** (R₁=Ph, R₂=4-THP) and the above aldehyde provided (R)-methyl 4-((6-methyl-5-((4-(2-oxo-5-phenyl-3-(tetrahydro-2H-pyran-4-yl)imidazolidin-1-yl)piperidin-1-yl)methyl)pyridin-2-yl)oxy)benzoate, which was treated under general procedure C to afford **6d** as a white solid (164 mg, 51% over two steps). ¹H NMR (300 MHz, CD₃OD) δ 1.32 (dq, 1H, J = 12.0, 3.6 Hz), 1.48 (br d, 1H, J = 12.0 Hz), 1.60–1.80 (m, 5H), 1.95–2.20 (m, 3H), 2.39 (s, 3H), 2.78 (d, 1H, J = 11.4 Hz), 2.94 (d, 1H, J = 11.1 Hz), 3.13 (m, 1H), 3.40–3.60 (m, 5H), 3.77 (t, 1H, J = 9.0 Hz), 3.93 (m, 3H), 4.73 (m, 1H), 6.69 (d, 1H, J = 8.1 Hz), 7.07 (d, 2H, J = 8.7 Hz), 7.30–7.40 (m, 5H), 7.64 (d, 1H, J = 8.4 Hz), 8.01 (d, 2H, J = 8.7 Hz). ¹³C NMR (75 MHz, CD₃OD) δ 20.71, 28.44, 29.82 (2C), 30.14, 48.57, 49.44, 52.08, 52.85, 53.05, 56.74, 57.98, 67.18, 67.27, 109.02, 119.53 (2C), 125.88, 127.02 (2C), 128.46, 129.03 (2C), 130.67, 131.50 (2C), 142.62, 142.91, 157.37, 158.09, 160.87, 162.01, 171.02. ES–MS *m/z* 571 [M + H]⁺. Anal. Calcd. for C₃₃H₃₈N₄O₅·0.7CH₂Cl₂·0.3NH₃: C, 63.38; H, 6.45; N, 9.87. Found: C, 63.20; H, 6.60; N, 9.85.

(R)-4-((5-((4-(5-(3-Chlorophenyl)-2-oxo-3-(tetrahydro-2H-pyran-4-yl)imidazolidin-1-yl)piperidin-1-yl)methyl)-6-methylpyridin-2-yl)oxy)benzoic Acid (6e). Following general procedure A, (R)-4-(3-chlorophenyl)-3-(piperidin-4-yl)-1-(tetrahydro-2H-pyran-4-yl)imidazolidin-2-one **10b** (R₁=Ph-3-Cl, R₂=4-THP) and methyl 4-((5-formyl-6-methylpyridin-2-yl)oxy)benzoate provided (R)-methyl 4-((5-((4-(5-(3-chlorophenyl)-2-oxo-3-(tetrahydro-2H-pyran-4-yl)imidazolidin-1-yl)piperidin-1-yl)methyl)-6-methylpyridin-2-yl)oxy)benzoate, which was treated under general procedure C to afford **6e** as a white solid (368 mg, 88% over two steps). ¹H NMR (300 MHz, CD₃OD) δ 1.42 (dq, 1H, J = 12.6, 3.9 Hz), 1.50–1.80 (m, 6H), 2.05 (dq, 1H, J = 12.6, 3.6 Hz), 2.30 (m, 2H), 2.41 (s, 3H), 2.93 (d, 1H, J = 11.7 Hz), 3.05 (d, 1H, J = 11.7 Hz), 3.11 (m, 1H), 3.47 (t, 2H, J = 11.7 Hz), 3.55 (m, 1H), 3.63 (s, 2H), 3.78 (t, 1H, J = 9.3 Hz), 3.94 (m, 3H), 4.56 (m, 1H), 6.75 (d, 1H, J = 8.1 Hz), 7.10 (d, 2H, J = 8.4 Hz), 7.30–7.42 (m, 4H), 7.69 (d, 1H, J = 8.4 Hz), 8.03 (d, 2H, J = 8.7 Hz). ¹³C NMR (75 MHz, CD₃OD) δ 22.48, 28.01, 30.27, 30.31, 30.44, 48.64, 49.19, 51.49, 53.07 (2C), 55.68, 58.16, 67.59 (2C), 109.31, 120.14 (2C), 125.27, 126.94, 128.03, 128.97, 130.65, 132.10 (2C), 135.22, 142.94, 144.99, 157.38, 158.77, 160.24, 161.99, 169.83, 174.11. ES–S

m/z 605 [M + H]⁺. Anal. Calcd. for C₃₃H₃₇N₄O₅·0.6CH₂Cl₂: C, 61.51; H, 5.87; N, 8.54. Found: C, 61.56; H, 5.82; N, 8.44.

(R)-4-((6-Ethyl-5-((4-(2-oxo-5-phenyl-3-(tetrahydro-2H-pyran-4-yl)imidazolidin-1-yl)piperidin-1-yl)methyl)pyridin-2-yl)oxy)benzoic Acid (6h). Following general procedure A, (R)-4-phenyl-3-(piperidin-4-yl)-1-(tetrahydro-2H-pyran-4-yl)imidazolidin-2-one **10b** (R₁=Ph, R₂=4-THP) and *t*-butyl 4-((6-ethyl-5-formylpyridin-2-yl)oxy)benzoate provided (R)-*t*-butyl 4-((6-ethyl-5-((4-(2-oxo-5-phenyl-3-(tetrahydro-2H-pyran-4-yl)imidazolidin-1-yl)piperidin-1-yl)methyl)pyridin-2-yl)oxy)benzoate, which was treated under general procedure B to afford **6h** as a white powder (71 mg, 59% over two steps). ¹H NMR (300 MHz, CDCl₃) δ 1.11 (t, 3H, J = 7.5 Hz), 1.25–1.42 (m, 2H), 1.66 (m, 5H), 2.14–2.28 (m, 3H), 2.88 (br, s, 1H), 3.08 (m, 2H), 3.48–3.81 (m, 5H), 4.01 (m, 3H), 4.59 (t, 1H, J = 7.5 Hz), 6.62 (d, 1H, J = 9.0 Hz), 7.05–7.26 (m, 5H), 7.14 (d, 2H, J = 9.0 Hz), 7.65 (br s, 1H), 8.02 (br s, 2H). ¹³C NMR (75 MHz, CDCl₃) δ 13.74, 28.01, 30.20, 30.52, 48.74, 49.14, 51.52, 52.96, 56.33, 57.64, 67.53, 67.62, 109.12, 120.24, 122.03, 127.09, 128.39, 128.72, 129.30, 131.97, 142.66, 142.88, 158.56, 160.33, 161.79, 162.07, 170.32. ES–MS *m/z* 585 [M + H]⁺. Anal. Calcd. for C₃₃H₄₀N₄O₅·0.5CH₂Cl₂: C, 66.07; H, 6.59; N, 8.93. Found: C, 66.02; H, 6.65; N, 8.91.

(R)-4-((5-((4-(2-Oxo-5-phenyl-3-(tetrahydro-2H-pyran-4-yl)imidazolidin-1-yl)piperidin-1-yl)methyl)pyridin-2-yl)thio)benzoic Acid (6i). 2-Bromo-5-methylpyridine (2.23 g, 13.0 mmol), 4-mercaptobenzoic acid (333 mg, 2.16 mmol), and K₂CO₃ (597 mg, 4.32 mmol) were heated at 200 °C for 2 h. The mixture was partitioned between H₂O (70 mL) and diethyl ether (20 mL). The aqueous phase was extracted with diethyl ether (20 mL) and then acidified to pH 3 with 10% HCl (aq). The aqueous phase was extracted with 10% MeOH/CH₂Cl₂ (4 × 20 mL), and the combined organic layers were dried (MgSO₄) and concentrated to give a yellow solid (412 mg). A solution of the yellow solid from above (412 mg) and H₂SO₄ (0.11 mL) in MeOH (16 mL) was heated to reflux for 15 h and then concentrated. The residue was dissolved in CH₂Cl₂ (15 mL), washed with H₂O (5 mL) and saturated NaHCO₃ (aq) (10 mL), dried (MgSO₄), and concentrated. Purification by chromatography on silica gel (0–5% EtOAc/CH₂Cl₂) gave methyl 4-((5-methylpyridin-2-yl)thio)benzoate as colorless crystals (280 mg, 50% over two steps), which was added to a mixture of NBS (231 mg, 1.30 mmol) and benzoyl peroxide (39 mg, 0.16 mmol) in CCl₄ (2.7 mL), heated to reflux for 4 h, and filtered and concentrated. Purification by chromatography on silica gel (1% EtOAc/CH₂Cl₂) gave methyl 4-((5-(bromomethyl)pyridin-2-yl)thio)benzoate as colorless crystals (161 mg, 44%). ¹H NMR (300 MHz, CDCl₃) δ 3.94 (s, 3H), 4.43 (s, 2H), 7.05 (d, 1H, J = 8.4 Hz), 7.56 (dd, 1H, J = 8.4, 2.4 Hz), 7.61 (dd, 2H, J = 6.6, 1.8 Hz), 8.06 (dd, 2H, J = 6.8, 1.7 Hz), 8.45 (d, 1H, J = 2.1 Hz). Following general procedure D, (R)-1-cyclohexyl-4-phenyl-3-(piperidin-4-yl)imidazolidin-2-one **10b** (R₁=Ph, R₂=4-THP) (80 mg, 0.24 mmol) and methyl 4-((5-(bromomethyl)pyridin-2-yl)thio)benzoate (75 mg) in CH₃CN (4 mL) afforded (R)-methyl 4-((5-((4-(2-oxo-5-phenyl-3-(tetrahydro-2H-pyran-4-yl)imidazolidin-1-yl)piperidin-1-yl)methyl)pyridin-2-yl)thio)benzoate as a white foam (105 mg, 81%). Following general procedure C, the ester prepared above (105 mg, 0.18 mmol) afforded **6i** as a white precipitate (64 mg, 62%). ¹H NMR (300 MHz, CDCl₃) δ 1.48 (br s, 1H), 1.64–1.74 (m, 4H), 1.86–1.90 (m, 1H), 2.53 (br s, 2H), 2.72 (br s, 1H), 3.12–3.21 (m, 2H), 3.43–3.52 (m, 4H), 3.70 (t, 1H, J = 9.3 Hz), 3.83–4.20 (m, 6H), 4.61–4.65 (m, 1H), 6.98 (d, 1H, J = 6.0 Hz), 7.19–7.31 (m, 6H), 7.60 (d, 2H, J = 8.1 Hz), 8.01 (d, 2H, J = 8.1 Hz), 8.30 (s, 1H). ¹³C NMR (75 MHz, CDCl₃) δ 25.7, 27.3, 29.8, 30.1, 48.3, 48.9, 49.3, 51.5, 53.5, 55.7, 67.1, 67.2, 122.0, 126.7, 128.6, 129.2, 131.0, 132.1, 134.4, 135.4, 140.0, 141.8, 151.1, 159.7, 162.5, 168.5. ES–MS *m/z* 573 [M + H]⁺. Anal. Calcd. for C₃₂H₃₆N₄O₄S·1.6CH₂Cl₂: C, 56.95; H, 5.58; N, 7.91. Found: C, 56.91; H, 5.90; N, 8.00.

(R)-4-((6-Methyl-5-((4-(2-oxo-5-phenyl-3-(tetrahydro-2H-pyran-4-yl)imidazolidin-1-yl)piperidin-1-yl)methyl)pyridin-2-yl)oxy)benzamide (6k). A mixture of 6-bromo-2-methylpyridine-3-carboxaldehyde (1.00 g, 5.00 mmol), 4-hydroxybenzamide (0.596 g, 5.00 mmol), and K₂CO₃ (0.414 g, 3.00 mmol) in DMF (10 mL) was heated at 130 °C for 1 h. The mixture was cooled to room

temperature, and DMF was removed. Aqueous workup and purification by flash chromatography on silica gel (EtOAc/hexanes, 2:3 in v/v) afforded 4-(5-formyl-6-methylpyridin-2-yloxy)benzotrile as a white solid (0.497 g, 41%). $^1\text{H NMR}$ (300 MHz, CDCl_3) δ 2.72 (s, 3H), 6.92 (d, 1H, $J = 8.4$ Hz), 7.28–7.31 (m, 2H), 7.69–7.73 (m, 2H), 8.17 (d, 1H, $J = 8.4$ Hz), 10.26 (s, 1H). Following general procedure A, (R)-1-cyclohexyl-4-phenyl-3-(piperidin-4-yl)-imidazolidin-2-one **10b** ($R_1 = \text{Ph}$, $R_2 = 4\text{-THP}$) (63 mg, 0.19 mmol) and the above aldehyde (55 mg, 0.23 mmol) afforded (R)-4-((6-methyl-5-((4-(2-oxo-5-phenyl-3-(tetrahydro-2H-pyran-4-yl)imidazolidin-1-yl)piperidin-1-yl)methyl)pyridin-2-yl)oxy)benzotrile as a white solid (56 mg, 53%). To a solution of the above nitrile (53 mg, 96 μmol) in TFA (2 mL) was added concd H_2SO_4 (4 drops). The reaction was heated at 95 $^\circ\text{C}$ for 16 h and then concentrated to dryness under reduced pressure. The crude residue was then purified by column chromatography on silica gel (25:1:0.1, $\text{CH}_2\text{Cl}_2/\text{MeOH}/\text{NH}_4\text{OH}$) to afford **6k** as a white solid (49 mg, 89%). $^1\text{H NMR}$ (300 MHz, CDCl_3) δ 1.22 (dq, 1H, $J = 12.0, 3.6$ Hz), 1.42 (d, 1H, $J = 12.0$ Hz), 1.67 (m, 5H), 1.92 (m, 2H), 2.04 (m, 1H), 2.38 (s, 3H), 2.64 (d, 1H, $J = 10.5$ Hz), 2.83 (d, 1H, $J = 9.3$ Hz), 3.07 (m, 1H), 3.32 (s, 2H), 3.46 (m, 2H), 3.61 (m, 1H), 3.63 (t, 1H, $J = 9.0$ Hz), 4.02 (m, 3H), 4.59 (m, 1H), 6.63 (d, 1H, $J = 8.1$ Hz), 7.14 (d, 2H, $J = 8.7$ Hz), 7.34 (s, 5H), 7.50 (d, 1H, $J = 8.1$ Hz), 7.82 (d, 2H, $J = 8.1$ Hz). ES–MS m/z [M + H] $^+$.

Cell Lines. The HEK293F human embryonic kidney cell line was obtained from the ATCC. The CHO-Tat-10 cell line constitutively expressing HIV-1 JRFLenv and HIV-1 Tat was obtained under license from the Gladstone Institute. The HeLa-CD4-LTR- β -gal and P4-CCR5 cell lines were obtained from the NIH AIDS Research and Reference Reagent Program. HEK293F cells were transfected to express CCR1, CCR2B, CXCR3, CCR4, or CCR5. These receptors were cloned from commercial cDNA libraries by PCR using published gene sequences and were inserted into the TOPO-pcDNA3.1 vector (Invitrogen). Cells expressing CCR4, CCR5, and CXCR3 were also cotransfected with a chimeric $\text{G}\alpha_{\text{qis}}$ protein to improve signaling. HEK293F cells were maintained in Dulbecco's modified Eagle's medium supplemented with 10% fetal bovine serum (FBS), 1 mM sodium pyruvate, 1 mM nonessential amino acids, and 4 mM L-glutamine. The CHO-Tat-10 cell line was maintained in RPMI 1640 media supplemented with 10% fetal bovine serum, 2 mM glutamine, 1 mM sodium pyruvate, 1 \times nonessential amino acids, 0.5 mg/mL Geneticin, and 12 $\mu\text{g}/\text{mL}$ puromycin. The HeLa-CD4-LTR- β -gal and P4-CCR5 cell lines were maintained in Dulbecco's modified Eagle's medium supplemented with 10% FBS, 4 mM glutamine, 1 mM sodium pyruvate, 1 \times nonessential amino acids, 0.2 mg/mL Geneticin, and 0.1 mg/mL hygromycin. All cell culture media and supplements were obtained from Hyclone Inc. with the exceptions of the fetal bovine serum, which was obtained from Invitrogen Inc., and hygromycin, which was obtained from Calbiochem. CCRF-CEM cells, which naturally express CXCR4 and CCR7, were cultured in RPMI 1640 supplemented with 1 mM sodium pyruvate, 2 mM L-glutamine and 10% FBS. CEM.NKR.CCR5 cells were obtained from NIH AIDS Research and Reagent program and grown in RPMI 1640 supplemented with 10% FBS and 4 mM L-glutamine.

Calcium Flux Assay. Chemokine-stimulated calcium flux was assayed as previously described.⁴⁹ Briefly, cells were washed and loaded with Fluo-4/AM (4 μM) (Molecular probes, Inc.) and washed and resuspended in Hanks' balanced salt solution in 20 mM HEPES, 0.2% BSA, 2.5 mM probenecid, pH 7.4. Cells were then preincubated with test compound for 15 min, and changes in the intracellular calcium concentration upon chemokine addition (RANTES (CCL5) for CCR5, MIP-1 α (CCL3) for CCR1, MCP-1 (CCL2) for CCR2b, TARC (CCL17) for CCR4, MIP-3 β (CCL19) for CCR7, SDF-1 α (CXCL12) for CXCR4, and IP10 (CXCL10) for CXCR3) were monitored using the FLEXstation (Molecular Devices) at 525 nm (excitation $\lambda = 485$ nm). Data were analyzed using the programs Softmax PRO 4.3.1 (Molecular Devices) and GraphPad Prism 3.0 software.

^{125}I -RANTES Binding Assay. The ^{125}I -RANTES binding assay was performed with membranes prepared from HEK293F cells expressing

wild-type CCR5.²⁶ CCR5 membranes were diluted in assay buffer to a concentration of 0.16–0.28 $\mu\text{g}/\mu\text{L}$ in a final volume of 50 μL . The ^{125}I -RANTES (PerkinElmer Life Sciences, 2200 Ci/mmol) was diluted to a final concentration of 50 pM. The membrane was incubated with 25 μL of ^{125}I -RANTES and 50 μL of buffer or compound over a concentration range of 1×10^{-5} to 6.4×10^{-10} M for 45 min at room temperature in Millipore Multiscreen plates with GF-B membranes (Millipore) blocked with 0.15% poly(ethyleneimine). The plates were washed three times with ice-cold 50 mM HEPES, 0.5 M NaCl, pH 7.4, dried, and counted on a Wallac 1450 Microbeta Jet liquid scintillation counter. Ligand binding dose/response curves were analyzed, and IC_{50} values were calculated using Prism 3.0 (GraphPad).

CCR5 Fusion Assay. A cell–cell fusion assay was used to mimic the first stage of the HIV infection process. The principle of the assay is the fusion of one cell line expressing the HIV-1 JRFL viral envelope protein and the Tat transcription factor (CHO-Tat10) with a second cell line (HeLa-CD4-LTR- β -gal) expressing CD4 and CCR5 and the *LacZ* gene under the control of the HIV-1 LTR promoter.

For compound screening, the P4-CCR5 cell line, which expresses CCR5, CD4, and a reporter gene, β -galactosidase, was used. The cells were washed by centrifugation and resuspended in fusion-assay medium (DMEM/RPMI 1640 1:1 supplemented with 10% FBS) and the concentration was adjusted to 0.4×10^6 cells/ml. Similarly, confluent CHO-Tat cells were washed with PBS, lifted with TEN buffer, and resuspended to a concentration of 0.4×10^6 cells/ml in assay medium. Stock solutions of all compounds were prepared in DMSO and subsequently diluted into the fusion-assay medium. Equal volumes of CCR5-expressing cells and CHO-Tat cells were then mixed just prior to plating, and 50 μL of the cell mixture was added to the wells of a 96-well plate. Fifty microliters of diluted compound was then added to the cells to give a final concentration range of either 1×10^{-5} to 6.4×10^{-10} M or 1×10^{-6} to 6.4×10^{-12} M. The plates were incubated for 20 h at 37 $^\circ\text{C}$, 5% CO_2 , and then assayed for β -galactosidase activity using the Gal-Screen homogeneous chemiluminescent reporter gene assay (Applied Biosystems). The plates were read on a Victor 2 plate reader. IC_{50} values were calculated using nonlinear regression curve fitting (ExcelFit 3.0).

HIV-1 Infection Assay. Human PBMCs were isolated from a fresh buffy coat (Blood Transfusion Center Leuven), cultured in RPMI 1640 medium supplemented with 10% FBS and 1% glutamine, and stimulated for 3 days with 2 $\mu\text{g}/\text{mL}$ of phytohemagglutinin (PHA). Next, 500 000 cells/well in 200 μL of medium were infected with R5 HIV-1 strains and isolates (500 pg of p-24 Ag virus/500 μL) and treated with 2.5 ng/mL of IL-2 (R&D Systems) and serial dilutions of the test compound (compounds were only given one time at the beginning of the assay) to give a final volume of 500 μL . The cells were treated with further IL-2 after 5 days. After 10 days of culture, the viral replication was assayed by measuring viral p-24 in the culture supernatant by P-24 Ag ELISA (PerkinElmer). Cell viability was assayed using the MTS assay. The IC_{50} for HIV-1 inhibition (concentration of compound causing 50% inhibition of viral replication) and the CC_{50} (the concentration causing 50% cell cytotoxicity) were calculated.

hERG Automated Patch-Clamp Assay. The hERG assay was performed at Genzyme in Waltham, MA. Chinese hamster ovary cells overexpressing the human cloned recombinant hERG channel were patch voltage clamped in the whole cell configuration using the parallel automated patch-clamp platform QPatch (Sopion Biosciences) according to the protocol described by the manufacturer. The external solution was composed of (in mM) 145 NaCl, 4 KCl, 2 CaCl_2 , 1 MgCl_2 , 10 HEPES, 10 Glucose, pH 7.4, ~ 300 mOsm. The internal solution was composed of (in mM) 120 KCl, 31.25 KOH, 5.4 CaCl_2 , 1.75 MgCl_2 , 10 EGTA, 10 HEPES, 4 $\text{Na}_2\text{-ATP}$, pH 7.2, ~ 290 mOsm. After a brief voltage step to -50 mV (to measure leak current) from a holding potential of -80 mV, channels were activated by a depolarizing voltage pulse to $+20$ mV for 5 s followed by a return of the voltage to -50 mV for 2 s. The peak amplitude of the characteristic deactivating hERG current was measured after subtracting the leak current measured prior to the step to $+20$ mV. The voltage protocol was applied every 10 s. Data was acquired at 1

kHz and was low-pass filtered through a 4-pole Bessel filter at 0.3 kHz. No compensation for series resistance was applied; however, on the basis of the low access resistances and current amplitudes, the voltage errors were negligible. The experiment protocol for control buffer (external solution to measure baseline current) or drug addition was preprogrammed on the QPatch software, and the assay proceeded automatically without user intervention. Each cell received, in increasing doses, six concentrations of the test compound. Each concentration was exposed to the cell for 120 s (12 current recordings per concentration), and the steady-state current levels after each concentration application were compared to the baseline values to generate the percent inhibition. Each test compound was tested in at least four different cells ($n \geq 4$). Data was fit to a Boltzmann function provided in the assay software.

Purkinje Fiber Action Potential. The hERG assay was used to predict toxicity as a result of cardiac arrhythmias caused by QT interval prolongation. However, the electrophysiology of the cardiac action potential (AP) involves several ion channels other than hERG; therefore, other techniques, such as the evaluation of AP in cardiac Purkinje fibers, may be required for evaluating proarrhythmic risk. The Purkinje fiber action potential assay was performed at ChanTest using isolated canine Purkinje fibers. Compounds were tested at a concentration of 10 μM ($n = 4$). Action-potential parameters were recorded at three different stimulation frequencies representing three basic cycle lengths (time between stimulating pulses) of 0.5, 1, and 2 s designed to simulate tachycardia (fast heart rate), normocardia (normal heart rate), and bradycardia (slow heart rate). The following parameters were recorded from the action potential trace: resting membrane potential (mV) (RMP), action-potential amplitude (mV) (APA), maximum rate of rise (V/s) (V_{max}), and action-potential duration at 60 and 90% repolarization (ms) (APD_{60} and APD_{90}). APD_{60} , APD_{90} , and V_{max} at each stimulus frequency are presented as percent change ($\Delta\%$) from baseline following application of the test article. RMP and APA data are presented as the change in membrane potential (ΔmV). Data are reported as the mean \pm SEM. Pooled data was tabulated for each condition: control baseline, test article concentration, and stimulus frequency. Changes in action-potential parameters were evaluated using one-way ANOVA followed by Dunnett's multiple comparison test (JMP Version 5, SAS Institute) to determine whether the change from baseline observed after equilibration with the test article concentration is significantly different ($P < 0.05$) from that observed in the vehicle control group.

PAMPA Assay. The parallel artificial membrane-permeation assay was used to assess the potential for oral absorption.⁵⁰ The principle of the assay is the passive diffusion of test compound through an artificial phospholipid bilayer on a filter support into an acceptor compartment. A 96-well acceptor plate was filled with 300 μL of 50 mM sodium phosphate, 5% DMSO. A filter plate was then placed on top of the acceptor plate, with the filters touching the liquid in the acceptor plate. Five microliters per well of lipid mixture consisting of 0.8% L- α -phosphatidylcholine, 0.8% L- α -phosphatidylethanolamine, 0.2% L- α -phosphatidylserine, 0.2% L- α -phosphatidylinositol, and 1% cholesterol in 1,7-octadiene was pipetted on to filter plate, and 150 μL of a 200 μM solution of test compound was added on top of the lipid layer. The plates were incubated for 16 h at 30 $^{\circ}\text{C}$. The compound concentration in the acceptor compartment was quantified by UV absorption and was used to calculate the apparent permeability, P_e .

■ ASSOCIATED CONTENT

📄 Supporting Information

Experimental procedures for all intermediates and select compounds **2c**, **3m**, **4c**, **4e–g**, **4p**, **5b**, **5d**, **5j**, **5p–q**, **6a–c**, **6f**, **6j**, **6l–n**, including ^1H NMR, ^{13}C NMR, and elemental analysis results. This material is available free of charge via the Internet at <http://pubs.acs.org>.

■ AUTHOR INFORMATION

Corresponding Author

*Phone 617-610-8624; E-mail: skere01@gmail.com.

Notes

The authors declare no competing financial interest.

■ ACKNOWLEDGMENTS

This work was supported by the KU Leuven GOA nos. 10/014 and PF/10/018. We thank all of our past colleagues in the Chemistry and Biology Departments of AnorMED Inc. (now Genzyme Corporation, a Sanofi company) for many fruitful discussions. We are grateful to Becky Provinciael, Sandra Claes, and Eric Fonteyn for excellent technical assistance.

■ ABBREVIATIONS USED

APD, action potential duration; AGP, α -1-acid glycoprotein; CC_{50} , concentration required to reduce the cell number by 50% compared to that for the untreated controls; CCR5, C-C-R Chemokine receptor 5; ECL 2, extracellular loop 2; gp120, envelope glycoprotein 120; HIV-1, Human immunodeficiency virus; IC_{90} , concentration at 90% inhibition; PBMC, peripheral blood mononuclear cell; RANTES, Regulated upon Activation, Normal T-cell Expressed, and Secreted

■ REFERENCES

- (1) Doranz, B. J.; Berson, J. F.; Rucker, J.; Doms, R. W. Chemokine receptors as fusion cofactors for human immunodeficiency virus type 1 (HIV-1). *Immunol. Res.* **1997**, *16*, 15–28.
- (2) Kwong, P. D.; Wyatt, R.; Robinson, J.; Sweet, R. W.; Sodroski, J.; Hendrickson, W. A. Structure of an HIV gp120 envelope glycoprotein in complex with the CD4 receptor and a neutralizing human antibody. *Nature* **1998**, *393*, 648–659.
- (3) Liu, R.; Paxton, W. A.; Choe, S.; Ceradini, D.; Martin, S. R.; Horuk, R.; MacDonald, M. E.; Stuhlmann, H.; Koup, R. A.; Landau, N. R. Homozygous defect in HIV-1 coreceptor accounts for resistance of some multiply-exposed individuals to HIV-1 infection. *Cell* **1996**, *86*, 367–377.
- (4) Samson, M.; Libert, F.; Doranz, B. J.; Rucker, J.; Liesnard, C.; Farber, C. M.; Saragosti, S.; Lapoumeroulie, C.; Cognaux, J.; Forceille, C.; Muyldermans, G.; Verhofstede, C.; Burtonboy, G.; Georges, T.; Imai, G.; Rana, S.; Yi, Y.; Smyth, R. J.; Collman, R. G.; Doms, R. W.; Vassart, G.; Parmentier, M. Resistance to HIV-1 infection in caucasian individuals bearing mutant alleles of the CCR-5 chemokine receptor gene. *Nature* **1996**, *382*, 722–725.
- (5) Kazmierski, W. M.; Aquino, C.; Chauder, B. A.; Deanda, F.; Ferris, R.; Jones-Hertzog, D. K.; Kenakin, T.; Koble, C. S.; Watson, C.; Wheelan, P.; Yang, H.; Youngman, M. Discovery of bioavailable 4,4-disubstituted piperidines as potent ligands of the chemokine receptor 5 and inhibitors of the human immunodeficiency virus-1. *J. Med. Chem.* **2008**, *512*, 6538–6546.
- (6) Habashita, H.; Kokubo, M.; Hamano, S.; Hamanaka, N.; Toda, M.; Shibayama, S.; Tada, H.; Sagawa, K.; Fukushima, D.; Maeda, K.; Mitsuya, H. Design, synthesis, and biological evaluation of the combinatorial library with a new spirodiketopiperazine scaffold. Discovery of novel potent and selective low-molecular-weight CCR5 antagonists. *J. Med. Chem.* **2006**, *49*, 4140–4152.
- (7) Palani, A.; Tagat, J. R. Discovery and development of small-molecule chemokine coreceptor CCR5 antagonists. *J. Med. Chem.* **2006**, *49*, 2851–2857.
- (8) Nishizawa, R.; Nishiyama, T.; Hisaichi, K.; Hirai, K.; Habashita, H.; Takaoka, Y.; Tada, H.; Sagawa, K.; Shibayama, S.; Maeda, K.; Mitsuya, H.; Nakai, H.; Fukushima, D.; Toda, M. Discovery of orally available spirodiketopiperazine-based CCR5 antagonists. *Bioorg. Med. Chem.* **2010**, *18*, 5208–5223.
- (9) Barber, C. G.; Blakemore, D. C.; Chiva, J.-Y.; Eastwood, R. L.; Middleton, D. S.; Paradowski, K. A. 1-Amido-1-phenyl-3-piperidinyl-

- butanes – CCR5 antagonists for the treatment of HIV: Part 1. *Bioorg. Med. Chem. Lett.* **2009**, *19*, 1075–1079.
- (10) Pryde, D. C.; Corless, M.; Fenwick, D. R.; Mason, H. J.; Stammen, B. C.; Stephenson, P. T.; Ellis, D.; Bachelor, D.; Gordon, D.; Barber, C. G.; Wood, A.; Middleton, D. S.; Blakemore, D. C.; Parsons, G. C.; Eastwood, R.; Platts, M. Y.; Statham, K.; Paradowski, K. A.; Burt, C.; Klute, W. The design and discovery of novel amide CCR5 antagonists. *Bioorg. Med. Chem. Lett.* **2009**, *19*, 1084–1088.
- (11) Barber, C. G.; Blakemore, D. C.; Chiva, J. Y.; Eastwood, R. L.; Middleton, D. S.; Paradowski, K. A. 1-Amido-1-phenyl-3-piperidinylbutanes – CCR5 antagonists for the treatment of HIV: Part 2. *Bioorg. Med. Chem. Lett.* **2009**, *19*, 1499–1503.
- (12) Duan, M.; Aquino, C.; Ferris, R.; Kazmierski, W. M.; Kenakin, T.; Koble, C.; Wheelan, P.; Watson, C.; Youngman, M. [2-(4-Phenyl-4-piperidinyl)ethyl]amine based CCR5 antagonists: Derivatizations at the N-terminal of the piperidine ring. *Bioorg. Med. Chem. Lett.* **2009**, *19*, 1610–1613.
- (13) Duan, M.; Aquino, C.; Dorsey, G. F., Jr.; Ferris, R.; Kazmierski, W. M. 4,4-Disubstituted cyclohexylamine based CCR5 chemokine receptor antagonists as anti-HIV-1 agents. *Bioorg. Med. Chem. Lett.* **2009**, *19*, 4988–4992.
- (14) Rotstein, D. M.; Gabriel, S. D.; Makra, F.; Filonova, L.; Gleason, S.; Brotherton-Pleiss, C.; Setti, L. Q.; Trejo-Martin, A.; Lee, E. K.; Sankuratri, S.; Ji, C.; deRosier, A.; Dioszegi, M.; Heilek, G.; Jekle, A.; Berry, P.; Weller, P.; Mau, C.-I. Spiropiperidine CCR5 antagonists. *Bioorg. Med. Chem. Lett.* **2009**, *19*, 5401–5406.
- (15) Lemoine, R. C.; Petersen, A. C.; Setti, L.; Wanner, J.; Jekle, A.; Heilek, G.; deRosier, A.; Ji, C.; Berry, P.; Rotstein, D. Evaluation of secondary amide replacements in a series of CCR5 antagonists as a means to increase intrinsic membrane permeability. Part 1: Optimization of gem-disubstituted azacycles. *Bioorg. Med. Chem. Lett.* **2010**, *20*, 704–708.
- (16) Lemoine, R. C.; Petersen, A. C.; Setti, L.; Baldinger, T.; Wanner, J.; Jekle, A.; Heilek, G.; deRosier, A.; Ji, C.; Rotstein, D. M. Evaluation of a 3-amino-8-azabicyclo[3.2.1]octane replacement in the CCR5 antagonist maraviroc. *Bioorg. Med. Chem. Lett.* **2010**, *20*, 1674–1678.
- (17) Rotstein, D. M.; Gabriel, S. D.; Manser, N.; Filonova, L.; Padilla, F.; Sankuratri, S.; Ji, C.; deRosier, A.; Dioszegi, M.; Heilek, G.; Jekle, A.; Weller, P.; Berry, P. Synthesis, SAR and evaluation of [1,40]-bipiperidinyl-4-yl-imidazolidin-2-one derivatives as novel CCR5 antagonists. *Bioorg. Med. Chem. Lett.* **2010**, *20*, 3219–3222.
- (18) Ben, Li.; Jones, E. D.; Zhou, E.; Li, C.; Baylis, D. C.; Yu, S.; Wang, M.; He, X.; Coates, J. A. V.; Rhodes, D. I.; Pei, G.; Deadman, J. J.; Xie, X.; Ma, D. Studies on the structure–activity relationship of 1,3,3,4-tetra-substituted pyrrolidine embodied CCR5 receptor antagonists. Part 1: Tuning the N-substituents. *Bioorg. Med. Chem. Lett.* **2010**, *20*, 4012–4014.
- (19) Chen, W.; Zhan, P.; De Clercq, E.; Liu, X. Recent progress in small molecule CCR5 antagonists as potential HIV-1 entry inhibitors. *Curr. Pharm. Des.* **2012**, *18*, 100–112.
- (20) Gulick, R. M.; Lalezari, J.; Goodrich, J.; Clumeck, N.; DeJesus, E.; Horban, A.; Nadler, J.; Clotet, B.; Karlsson, A.; Wohlfeiler, M.; Montana, J. B.; McHale, M.; Sullivan, J.; Ridgway, C.; Felstead, S.; Dunne, M. W.; Van der Ryst, E.; Mayer, H. Maraviroc for previously treated patients with R5 HIV-1 infection. *N. Engl. J. Med.* **2008**, *359*, 1429–1441.
- (21) HIVandHepatitis.com Home Page. http://www.hivandhepatitis.com/recent/2010/0716_2010_b.htm. (accessed August 18th, 2013).
- (22) Crabb, C. GlaxoSmithKline ends aplaviroc trials. *AIDS* **2006**, *20*, 641.
- (23) Skerlj, R.; Bridger, G.; Zhou, Y.; Bourque, E.; Langille, J.; Di Fluri, M.; Bogucki, D.; Yang, W.; Li, T.; Wang, L.; Nan, S.; Baird, I.; Metz, M.; Darkes, M.; Labrecque, J.; Lau, G.; Fricker, S.; Huskens, D.; Schols, D. Design and synthesis of pyridin-2-ylloxymethylpiperidin-1-ylbutyl amide CCR5 antagonists that are potent inhibitors of m-tropic (R5) HIV-1 replication. *Bioorg. Med. Chem. Lett.* **2011**, *21*, 2450–2455.
- (24) Skerlj, R.; Bridger, G.; Zhou, Y.; Bourque, E.; McEachern, E.; Langille, J.; Harwig, C.; Veale, D.; Yang, W.; Li, T.; Zhu, Y.; Bey, M.; Baird, I.; Sartori, M.; Metz, M.; Mosi, R.; Nelson, K.; Bodart, V.; Wong, R.; Fricker, S.; MacFarland, R.; Huskens, D.; Schols, D. Design and synthesis of pyridin-2-ylmethylaminopiperidin-1-ylbutyl amide CCR5 antagonists that are potent inhibitors of m-tropic (R5) HIV-1 replication. *Bioorg. Med. Chem. Lett.* **2011**, *21*, 6950–6954.
- (25) Skerlj, R.; Bridger, G.; Zhou, Y.; Bourque, E.; McEachern, E.; Danthi, S.; Langille, J.; Harwig, C.; Veale, V.; Carpenter, B.; Ba, T.; Bey, M.; Baird, I.; Wilson, T.; Metz, M.; MacFarland, R.; Mosi, R.; Bodart, V.; Wong, R.; Fricker, S.; Huskens, D.; Schols, D. Mitigating hERG Inhibition: Design of orally bioavailable CCR5 antagonists as potent inhibitors of R5 HIV-1 replication. *ACS Med. Chem. Lett.* **2012**, *3*, 216–221.
- (26) Labrecque, J.; Metz, M.; Lau, G.; Darkes, M.; Wong, R.; Bogucki, D.; Carpenter, B.; Chen, G.; Li, T.; Nan, S.; Schols, D.; Bridger, G. J.; Fricker, S. P.; Skerlj, R. T. HIV-1 entry inhibition by small-molecule CCR5 antagonists: A combined molecular modeling and mutant study using a high-throughput assay. *Virology* **2011**, *413*, 231–243.
- (27) Billic, E.; Seibert, C.; Pugach, P.; Ketas, T.; Trkola, A.; Endres, M. J.; Murgolo, N. J.; Coates, E.; Reyes, G. R.; Baroudy, B. M.; Sakmar, T. P.; Moore, J. P.; Kuhmann, S. E. The differential sensitivity of human and rhesus macaque CCR5 to small-molecule inhibitors of human immunodeficiency virus type 1 entry is explained by a single amino acid difference and suggests a mechanism of action for these inhibitors. *J. Virol.* **2004**, *78*, 4134–4144.
- (28) Castonguay, L. A.; Weng, Y.; Adolfsen, W.; Di Salvo, J.; Kilburn, R.; Caldwell, C. G.; Daugherty, B. L.; Finke, P. E.; Hale, J. J.; Lynch, C. L.; Mills, S. G.; MacCoss, M.; Springer, M. S.; DeMartino, J. A. Binding of 2-aryl-4-(piperidin-1-yl)butanamines and 1,3,4-trisubstituted pyrrolidines to human CCR5: A molecular modeling-guided mutagenesis study of the binding pocket. *Biochemistry* **2003**, *42*, 1544–1550.
- (29) Dragic, T.; Trkola, A.; Thompson, D. A.; Cormier, E. G.; Kajumo, F. A.; Maxwell, E.; Lin, S. W.; Ying, W.; Smith, O. S.; Sakmar, T. P.; Moore, J. P. A binding pocket for a small molecule inhibitor of HIV-1 entry within the transmembrane helices of CCR5. *Proc. Natl. Acad. Sci. U.S.A.* **2000**, *97*, 5639–5644.
- (30) Kondru, R.; Zhang, J.; Ji, C.; Mirzadegan, T.; Rotstein, D.; Sunkurati, S.; Dioszegi, M. Molecular interactions of CCR5 with major classes of small-molecule anti-HIV CCR5 antagonists. *Mol. Pharmacol.* **2008**, *73*, 789–800.
- (31) Maeda, K.; Das, D.; Ogata-Aoki, H.; Nakata, H.; Miyakawa, T.; Tojo, Y.; Norman, R.; Takaoka, Y.; Ding, J.; Arnold, E.; Mitsuya, H. Structural and molecular interactions of CCR5 inhibitors with CCR5. *J. Biol. Chem.* **2006**, *281*, 12688–12698.
- (32) Nishikawa, M.; Takashima, K.; Nishi, T.; Furuta, R. A.; Kanzaki, N.; Yamamoto, Y.; Fujisawa, J.-I. Analysis of binding sites for the new small-molecule CCR5 antagonists TAK-220 on human CCR5. *Antimicrob. Agents Chemother.* **2005**, *49*, 4708–4715.
- (33) Seibert, C.; Ying, W.; Gavrillo, S.; Tsamis, F.; Kuhmann, S. E.; Palani, A.; Tagat, J. R.; Clader, J. W.; McCombie, S. W.; Baroudy, B. M.; Smith, S. O.; Dragic, T.; Moore, J. P.; Sakmar, T. P. Interaction of small molecule inhibitors of HIV-1 entry with CCR5. *Virology* **2006**, *349*, 41–54.
- (34) Stuppel, P. A.; Batchelor, D. V.; Corless, M.; Dorr, P. K.; Ellis, D.; Fenwick, D. R.; Galan, S. R. G.; Jones, R. M.; Mason, H. J.; Middleton, D. S.; Perros, M.; Perruccio, F.; Platts, M. Y.; Pryde, D. C.; Rodrigues, D.; Smith, N. N.; Stephenson, P. T.; Webster, R.; Westby, M.; Wood, A. An imidazopiperidine series of CCR5 antagonists for the treatment of HIV: The discovery of N-((1S)-1-(3-fluorophenyl)-3-((3-endo)-3-(S-isobutanyl-2-methyl-4,5,6,7-tetrahydro-1H-imidazo[4,5-c]pyridine-1-yl)-8-azabicyclo[3.2.1]oct-8-yl)propyl)acetamide (PF-232798). *J. Med. Chem.* **2011**, *54*, 67–77.
- (35) Tsamis, F.; Gavrillo, S.; Kajumo, F.; Seibert, C.; Kuhmann, S.; Ketas, T.; Trkola, A.; Palani, A.; Clader, J. W.; Tagat, J. R.; McCombie, S.; Baroudy, B.; Moore, J. P.; Sakmar, T. P.; Dragic, T. Analysis of the mechanism by which the small-molecule CCR5 antagonists SCH-

351125 and SCH-350581 inhibit human immunodeficiency type 1 entry. *J. Virol.* **2003**, *77*, 5201–5208.

(36) Kazmierski, W. M.; Anderson, D. L.; Aquino, C.; Chauder, B. A.; Duan, M.; Ferris, R.; Kenakin, T.; Koble, C. S.; Lang, D. G.; McIntyre, M. S.; Peckman, J.; Watson, C.; Wheelan, P.; Spaltenstein, A.; Wire, M. B.; Svolt, A.; Youngman, M. Novel 4,4-disubstituted piperidine-based C-C chemokine receptor-5 inhibitors with high potency against human immunodeficiency virus-1 and an improved human ether-a-go-go related gene (hERG) profile. *J. Med. Chem.* **2011**, *54*, 3756–3767.

(37) Price, D. A.; Armour, D.; de Groot, M.; Leishman, D.; Napier, C.; Perros, M.; Stammen, B. L.; Wood, A. Overcoming hERG affinity in the discovery of the CCR5 antagonist maraviroc: A CCR5 antagonist for the treatment of HIV. *Curr. Top. Med. Chem.* **2008**, *8*, 1140–1151.

(38) Schols, D.; Struyf, S.; Van Damme, J.; Este, J. A.; Henson, G.; De Clercq, E. Inhibition of t-tropic HIV strains by selective antagonization of the chemokine receptor CXCR4. *J. Exp. Med.* **1997**, *186*, 1383–1388.

(39) O'Brien, P.; Osborne, S. A.; Parker, D. D. Asymmetric aminohydroxylation of substituted styrenes: Applications in the synthesis of enantiomerically enriched arylglycinols and a diamine. *J. Chem. Soc., Perkin Trans.* **1998**, *1*, 2519–2526.

(40) Zhou, Y.; Bourque, E.; Zhu, Y.; McEachern, E.; Harwig, C.; Skerlj, R.; Bridger, G.; Li, T.; Metz, M. Chemokine receptor binding compounds. WO 2007/022371 A2.

(41) Palani, A.; Shapiro, S.; Clader, J. W.; Greenlee, W. J.; Cox, K.; Strizki, J.; Endres, M.; Baroudy, B. M. Discovery of 4-[(Z)-(4-bromophenyl)-(ethoxyimino)methyl]-1'-[(2,4-dimethyl-3-pyridinyl)carbonyl]-4'-methyl-1,4'-bipiperidine N-oxide (SCH 351125): An orally bioavailable human CCR5 antagonist for the treatment of HIV infection. *J. Med. Chem.* **2001**, *44*, 3339–3342.

(42) Walters, I.; Bennion, C.; Connolly, S.; Croshaw, P. J.; Hardy, K.; Hartopp, P.; Jackson, C. G.; King, S. J.; Lawrence, L.; Mete, A.; Murray, D.; Robinson, D. H.; Stein, L.; Wells, E.; Withnall, W. J. Synthesis and evaluation of substrate-mimicking cytosolic phospholipase A₂ inhibitors – reducing the lipophilicity of the arachidonyl chain isostere. *Bioorg. Med. Chem. Lett.* **2004**, *14*, 3645–3650.

(43) Veber, D. F.; Johnson, S. R.; Cheng, H. Y.; Smith, B. R.; Ward, K. W.; Kopple, K. D. Molecular properties that influence the oral bioavailability of drug candidates. *J. Med. Chem.* **2002**, *45*, 2615–2623.

(44) Metz, M.; Bourque, E.; Labrecque, J.; Danthi, S. J.; Langille, J.; Harwig, C.; Yang, W.; Darkes, M. C.; Lau, G.; Santucci, Z.; Bridger, G. J.; Schols, D.; Fricker, S. P.; Skerlj, R. T. Prospective CCR5 small molecule antagonist compound design using a combined mutagenesis/modeling approach. *J. Am. Chem. Soc.* **2011**, *131*, 16477–16485.

(45) Bourque, E.; Metz, M.; Baird, L.; Yang, W.; Bridger, G.; Skerlj, R. Chemokine receptor binding compounds. WO 2008/070758 A1.

(46) Chvatchko, Y.; Hoogewerf, A. J.; Meyer, A.; Alouani, S.; Juillard, P.; Buser, R.; Conquet, F.; Proudfoot, A. E. I.; Wells, T. N. C.; Power, C. A. A key role for CC chemokine receptor 4 in lipopolysaccharide-induced endotoxic shock. *J. Exp. Med.* **2000**, *191*, 1755–1763.

(47) Schuh, J. M.; Power, C. A.; Proudfoot, A. E.; Kunkel, S. L.; Lukacs, N. W.; Hogaboam, C. M. Airway hyperresponsiveness, but not airway remodeling, is attenuated during chronic pulmonary allergic responses to *Aspergillus* in CCR4[±] mice. *FASEB J.* **2002**, *16*, 1313–1315.

(48) Allegretti, M.; Cesta, M. C.; Garin, A.; Proudfoot, A. E. I. Current status of chemokine receptor inhibitors in development. *Immunol. Lett.* **2012**, *145*, 68–78.

(49) Fricker, S. P.; Anastassov, V.; Cox, J.; Darkes, M. C.; Grujic, O.; Idzan, S. R.; Labrecque, J.; Lau, G.; Mosi, R. M.; Nelson, K. L.; Quin, L.; Santucci, Z.; Wong, R. S. Characterization of the molecular pharmacology of AMD3100: A specific antagonist of the G-protein coupled chemokine receptor, CXCR4. *Biochem. Pharmacol.* **2006**, *72*, 588–596.

(50) Sugano, K.; Hamada, H.; Machida, M.; Ushio, H. High throughput prediction of oral absorption: Improvement of the composition of the lipid solution used in parallel artificial membrane permeation assay. *J. Biomol. Screening* **2001**, *6*, 189–196.